INSTITUTO SUPERIOR DE ENGENHARIA DO PORTO
MESTRADO EM BIORRECURSOS




Desenvolvimento de uma célula de biocombustível enzimática de glicose / oxigénio baseada em transdutores de minas de grafite

MIGUEL ÂNGELO LOPES TAVARES
Julho de 2020

P.PORTO

Development of a membraneless enzymatic glucose/O_2 biofuel cell based on pencil graphite transducers

Dissertation subjected as a partial requirement to

obtain the master´s degree in Bioresources

Miguel Ângelo Lopes Tavares

Supervisor: Simone Morais (REQUIMTE-LAQV, Instituto Superior de Engenharia)

Co-Supervisor: Álvaro Torrinha (REQUIMTE-LAQV, Instituto Superior de Engenharia)

Porto

July 2020

This study was financially supported by the European Union (FEDER funds through COMPETE) and National Funds (*Fundação para a Ciência e Tecnologia-FCT*) through PTDC/ASP-PES/29547/2017 (POCI-01-0145-FEDER) by FCT/MEC with national funds and co-funded by FEDER.

Abstract

Nowadays, society is heavily dependent on multiple types of energy that are spent in numerous applications. Most of this energy is derived from non-renewable sources such as nuclear and fossil fuels that may represent serious environmental, social and economic concerns. The future of energy supply depends on the innovative design of green, sustainable, and efficient systems for the conversion of clean and readily available energy sources.

Biofuel cell is a sustainable, micro-energy production technology with promising applications in the biotechnological field and small consumable electronics. It is based on the application of biological entities such as microorganisms or enzymes in electrochemical transducers to convert the chemical energy of specific compounds into electrical signals. Particularly, enzymatic glucose/O_2 biofuel cells have been widely studied due to their promising implantable applications since energy can be extracted from biological fluids to power critical devices such as pacemakers.

The main objective of this work was the development of an enzymatic glucose/O_2 biofuel cell using low-cost pencil graphite electrodes (PGE) for the enzymatic transduction. Bioanode was based on the immobilization of glucose oxidase (GOx) enzyme for catalysis of glucose fuel while biocathode was based on the immobilization of bilirubin oxidase (BOx) enzyme for reduction of the oxidant O_2.

The experimental work began with the electrochemical characterization of PGE and comparison with conventional electrodes. Good voltammetric results were obtained for PGE in terms of cathodic/anodic peak intensities, peak-to-peak separation (ΔE_p) and electron transfer rate constant (k^0) justifying therefore their selection as a transducer for the immobilization of enzymes. In order to improve the electrochemical performance of PGE, nanostructuration of the electrode surface was assessed using different carbon nanomaterials (multi-walled carbon nanotubes (MWCNTs), single-walled carbon nanotubes (SWCNTs), reduced graphene (rGO)) through cyclic voltammetry (CV).

Prior to biofuel cell assembly, the biocathode and the bioanode were individually characterized as biosensors for the respective enzyme substrates. Therefore, the bioelectrode for O_2 was first developed by immobilizing BOx into a previously modified PGE (PGE-rGO-MWCNTs) using a pyrene-based succinimidyl ester (PBSE) cross-linker. After assessing enzyme immobilization by CV, O_2 was detected by amperometry achieving a sensitivity of 600 $\mu A.mM^{-1}.cm^{-2}$ and a limit of detection of 0.1 mM. When applied as a biocathode, the polarization curves resulted in an open circuit potential (OCP) of 0.52 V vs Ag/AgCl and generated a maximum current density of 170 $\mu A.cm^{-2}$ in the presence of O_2. The bioelectrode for glucose was fabricated in a similar way, however, using SWCNTs instead of MWCNTs (PGE-rGO-SWCNTs-PBSE-GOx). Although being efficiently immobilized in the electrode surface enabling direct electron transfer, the amperometric analysis revealed some instability and unreproducible problems, requiring the use of a mediator to facilitate the electron transfer between the enzyme and the electrode. In this mediated condition the sensitivity achieved was 55 $\mu A.mM^{-1}.cm^{-2}$ and the limit of detection was 0.09 mM.

Finally, the GOx and BOx bioelectrodes were assembled as bioanode and biocathode in a glucose /O_2 biofuel cell. In mediated electron transfer conditions, the membraneless biofuel cell achieved an OCP of 0.45 V and generated a power density of 26 µw.cm $^{-2}$. A membraneless glucose/O_2 biofuel cell was therefore successfully fabricated though requiring the use of a diffusional mediator to achieve maximum power.

Keywords: Biofuel cell, Biosensors, Enzymes, Carbon nanomaterials, Pencil graphite electrodes.

Resumo

Atualmente, a sociedade depende fortemente de vários tipos de energia que são usados em inúmeras aplicações. A maior parte dessa energia é derivada de fontes não renováveis, como combustíveis nucleares e fósseis, que podem apresentar sérias preocupações ambientais, sociais e económicas. O futuro do fornecimento energético depende do desenvolvimento inovador de sistemas verdes, sustentáveis e eficientes que possam ser empregues para a conversão de fontes de energia limpas e prontamente disponíveis.

As células de biocombustível são uma tecnologia sustentável de produção de microenergia, com aplicações no campo biotecnológico e em pequenos aparelhos eletrónicos. Baseia-se na aplicação de entidades biológicas, como microrganismos ou enzimas, em transdutores eletroquímicos para converter a energia química de compostos específicos em sinais elétricos. Particularmente, as células de biocombustível enzimáticas de glicose/O_2 têm sido amplamente estudadas devido a suas promissoras aplicações para dispositivos implantáveis, uma vez que a energia pode ser extraída de fluidos biológicos para alimentar dispositivos críticos como *pacemakers*.

O principal objetivo deste trabalho foi desenvolver uma célula de biocombustível enzimática de glicose/O_2 utilizando elétrodos de minas de grafite (PGE) de baixo custo para a transdução enzimática. O bioânodo baseia-se na imobilização da enzima glicose oxidase (GOx) para a catálise do combustível glicose, enquanto o biocátodo baseia-se na imobilização da enzima bilirrubina oxidase (BOx) para redução do oxidante O_2.

O trabalho experimental começou com a caracterização eletroquímica do PGE e a sua comparação com elétrodos convencionais. Foram obtidos bons resultados voltamétricos para o PGE no que diz respeito às intensidades do pico catódico/anódico, à separação pico-a-pico (ΔEp) e à constante de transferência de eletrões (k_0) justificando, portanto, a sua seleção como transdutor para a imobilização de enzimas. A fim de melhorar o desempenho eletroquímico do PGE, foi avaliada a nanoestruturação da superfície do elétrodo ao usar diferentes nanomateriais de carbono (nanotubos de carbono de superfície múltipla (MWCNTs), nanotubos de carbono de parede simples (SWCNTs), grafeno reduzido (rGO)) recorrendo à voltametria cíclica (CV).

Antes da construção da células de biocombustível, o biocátodo e o bioânodo foram caracterizados individualmente como biossensores para os respetivos substratos enzimáticos. O bioelétrodo para o O_2 foi desenvolvido inicialmente ao imobilizar a BOx num PGE previamente modificado (PGE-rGO-MWCNTs), utilizando um composto succinimidil-éster derivado do pireno (PBSE). Após avaliar a sua imobilização enzimática por CV, o O_2 foi detetado por amperometria, obtendo-se uma sensibilidade de 600 $\mu A.mM^{-1}.cm^{-2}$ e um limite de deteção de 0,1 mM. Ao aplicar como biocátodo, as curvas de polarização resultaram num potencial de circuito aberto (OCP) de 0,52 V *vs.* Ag / AgCl e produziram uma densidade de corrente máxima de 170 $\mu A.cm^{-2}$ na presença de O_2. O bioelétrodo para glicose foi construído de maneira semelhante, no entanto, usando SWCNTs em vez de MWCNTs (PGE-rGO-SWCNTs-PBSE-GOx). Embora a imobilização da enzima na superfície do elétrodo tenha sido eficaz, o que permitiu a transferência direta de eletrões, a análise por amperometria revelou alguns

problemas como falta de reprodutibilidade, o que exigiu o uso de um mediador para facilitar a transferência de eletrões entre a enzima e o elétrodo. Em condições mediadas, obteve-se uma sensibilidade de 55 $\mu A.mM^{-1}.cm^{-2}$ e um limite de deteção de 0,09 mM.

Por fim, os bioelétrodos com GOx e BOx foram montados como bioânodo e biocátodo numa célula de biocombustível de glicose/O_2 sem membrana. Em condições mediadas de transferência de eletrões, a célula de biocombustível sem membrana alcançou um OCP de 0,45 V e produziu uma densidade de potência de 26 $\mu w.cm^{-2}$. A célula de biocombustível de glicose/O_2 sem membrana foi construída com sucesso, embora esta exija o uso de um mediador difusional para se obter a potência máxima.

Palavras-chave: Células de biocombustível, Biossensores, Enzimas, Nanomateriais de Carbono, Elétrodos de Minas de Grafite.

General Index

Figure Index

Table Index

1. Literature Review

1.1. General Introduction

Energy may be the most important factor that will influence the shape of society in the 21st century. The cost and availability of energy significantly impact our quality of life, the health of economies and the environment stability. Societies have depended on different types of energy in the past and they have been forced to change from one energy type to another [1].

Energy demand is continuously growing as emerging economies become more prosperous and advanced. Estimations point out that in 2050 the world population will reach 9 billion, an almost 30% increment and with it, we can also expect an increase in resource harvesting. Currently, non-renewable energy sources such as fossil fuels and nuclear energy represent about 80% of the total energy consumption by source, whereas renewable energy represents only 11% (Figure 1) [2].

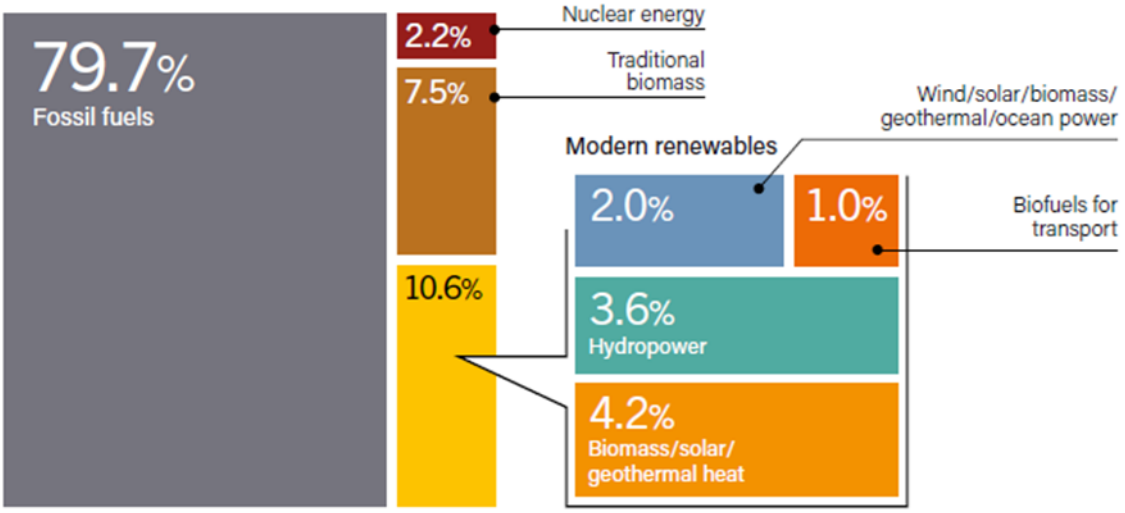

Figure 1- Estimated Renewable Share of Total Final Energy Consumption, 2017 [2].

The CO_2 emissions are mostly originated from the combustion of fossil fuels such as oil, coal and natural gas and biomass as a consequence of the energy-intensive human activities [2]. These are efficient fuels since they have high specific energy with the capability to produce high specific power. Unfortunately, the conversion of these fuels into energy through combustion releases high amounts of environmentally harmful substances such as carbon dioxide-based (CO_x) and nitrous oxide-based (NO_x) gases, the so-called, greenhouse gases which consequently affects world climate through severe climate changes [3].

The future of energy supply depends on the innovative design of green, sustainable, and efficient systems for the conversion of clean and cheap energy sources [4].

Current energy production systems from renewable sources possess low conversion efficiency, nevertheless, they benefit from the fact that they can be installed in non-usable or non-profitable space. For instance, solar energy can be harvested in deserts, building rooftops and

facades while wind energy is currently harvested from turbines installed in mountains and ocean and the same happen with tidal energy [5]. Currently, no individual renewable energy source has the ability to compete with and replace the conventional fossil-fuel-based energy generation approach, however, combining renewable energy may be alternative routes to be explored [6].

In order to attain world energy demand but meeting at the same time the goal of "net-zero" CO_2 emissions by 2050 as advised in the report from The Intergovernmental Panel on Climate Change (IPCC) [7], it is imperative to continue the investment in the current renewable energy technologies. More importantly, is the necessity in the development of new environmentally friendly and sustainable technologies. Biofuel cells (BFC) are seen as sustainable technology in the field of micro-energy production. Since the power produced range in the microwatt (μW) to milliwatt (mW) level, obviously biofuel cells will not resolve the energy problem, nonetheless, promising applications for this technology is envisaged in the near future as will be discussed later [8].

In general terms, fuel cells convert chemical energy (fuel) into electrical energy through redox reactions by using two connected electrodes designated as anode and cathode. At the anode occurs the oxidation of the fuel and the generated electrons move to the cathode in the external circuit where occurs a reduction of an oxidant. At the cathode, both electrons and protons combine with oxygen to form water. Concomitantly, protons diffuse from the anolyte to the catholyte, which are separated by a membrane in order to prevent cross-reactions (Figure 2). In a traditional way, fuel cells operate using relatively simple inorganic compounds like hydrogen, methanol, lower-order alcohols and alkanes. In Fuel cells, fuel and oxidant can be continuously supplied to the system differing from batteries which are closed systems [8; 9].

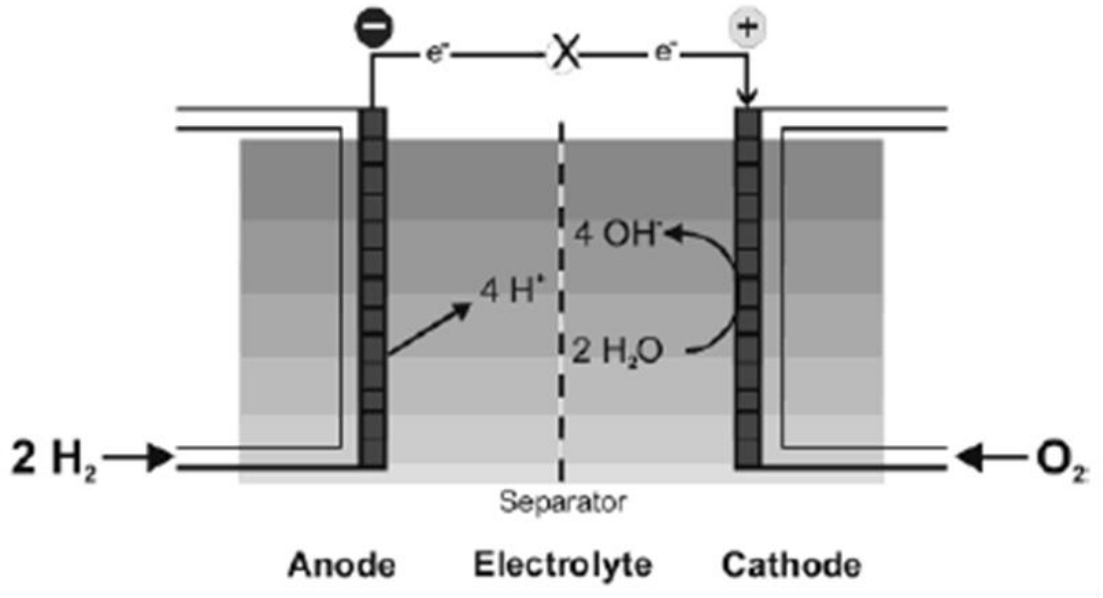

Figure 2- Schematic presentation of the working principles of a typical hydrogen/oxygen fuel cell [8].

Fuel cells may present some environmental issues [9]:

- Require the use of noble metals based catalysts, such as platinum, which are expensive;
- The catalysts are also poisoned by carbon monoxide impurities and their removal add more costs to the process;
- Require the use of acidic or basic electrolytes and they operate at higher temperatures conditions;
- Usually are more spacious and require a membrane as a separator between anode and cathode compartments.

The study and development of new fuel cell systems are necessary to improve the efficiency and productivity in comparison with more conventional technologies. As a result, Biofuel cell technology was created.

1.2.Biofuel Cells Characteristics

BFC are defined (in a broad sense) as devices capable of transforming chemical energy into electrical energy via electrochemical reactions involving biochemical pathways. In a simple way, the fuel is being combusted in a simple reaction without the formation of heat. BFC can have simple compounds such as hydrogen/methane or more complex as sugar, hydrocarbons or other carbon sources as fuels [10].

There are 3 different types of biofuel cells: enzymatic biofuel cells, microbial biofuel cells, and mammalian biofuel cells. The main difference between all is the catalysts in use (Table 1). Those catalysts can be applied to both electrodes or just one electrode (half-catalyst) or disperse on the electrolyte [11].

Table 1- Different types of Biofuel cells, based on [9].

Type of Biofuel Cell	**Enzymatic**	**Microbial**	**Mammalian**
Catalyst	Isolated Enzymes	Microorganism (whole or part of)	Mammalian Cells (whole or part of)

The Enzymatic, Microbial, and Mammalian Biofuel cells use organic catalysts in their assembly (Figure 3). These organic catalysts add specificity and selectivity towards their substrates, avoiding, therefore, interferences in the occurring reactions. This important feature makes possible the mixture of fuel and oxidant, eliminating the need for a membrane that separates anolyte (solution containing the fuel) and catholyte (solution containing the oxidant). In some

cases, the biocatalysts may require a mediator to facilitate the electron transfer with the electrode surface, due to the internal resistance of the organic catalyst and electrolyte [12].

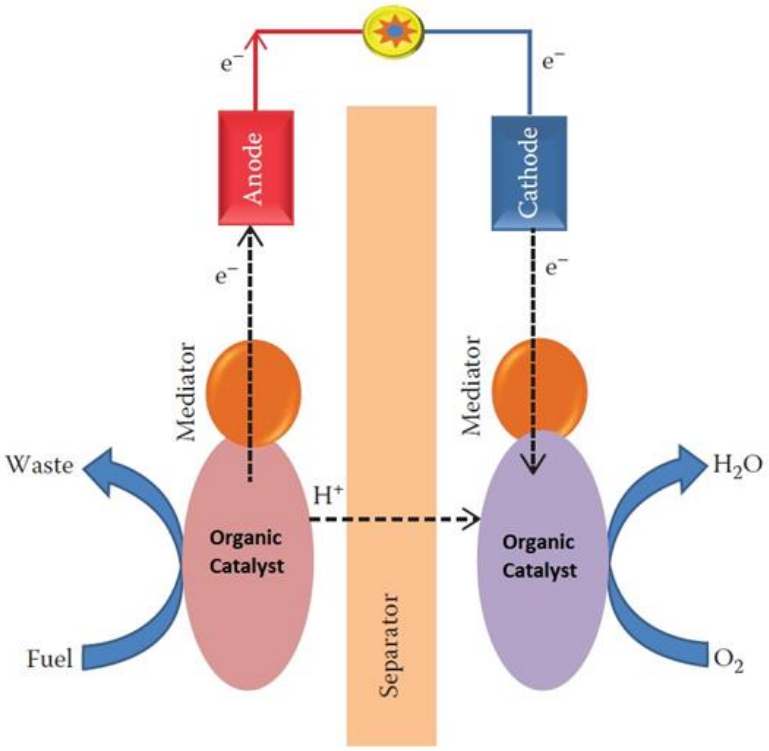

Figure 3- Schematic of a biofuel cell, adapted from [9].

The combination between biocatalysts and an electrode can be named as electrochemical biosensors that can be defined as a self-contained and integrated device that uses a biological recognition element (biochemical receptor) in direct spatial contact with an electrochemical transducer to produce certain quantitative or semiquantitative analytical information on an analyte of interest [13]. A further connection between two different electrochemical biosensors (one that catalyzes oxidation and the other reduction) originates a biofuel cell.

The major disadvantages of biofuel cells are the limited lifetime of biocatalysts and the lower power density generated per unit electrode surface area. Researchers have focused on some possibilities as solutions such as the right immobilization of the biocatalyst on the electrode, genetic engineering to modify and optimize the organic catalyst for better performance and stability [14].

Between all of biofuel cell types, enzymatic biofuel cells (EFCs) are the most promising when considering biocompatibility, selectivity, efficiency, and sensitivity criteria. EFCs typically produce higher power densities (although still lower than conventional fuel cells) when compared to microbial biofuel cells, but can only partially oxidize the fuel and have limited lifetimes (typically 7–10 days) owing to the fragile nature of the enzyme [14; 15]. The characteristics of enzymes used in fuel cells and biosensors will be discussed in more detail later in this work.

1.3.Biofuel Cells Applications

A wide range of applications of Biofuel cells has been proposed in recent years. Biofuels are extremely flexible, reliable and adaptable to a diverse number of applications, such as [16]:

- Transport and energy generation;
- Implantable power sources;
- Energy generation from wastes;
- Clinical diagnosis and environmental analysis;
- Energy supplier for Robotics and small electronics.

Biofuel cells offer the possibility of generating energy from renewable sources (such as carbo-based sources), which many are available in waste and by-products generated from processing industries [16].

As the biofuel cell can operate without a membrane separator, is it possible to produce low-size scale BFCs. Those BFCs can be implantable in living humans and animals as a self-powered biosensor for *in-situ* analyses [16]. Potentially, devices such as these could continuously monitor glucose levels in diabetes sufferers or to detect essential compounds like oxygen [17]. Also, is possible to create an automated system that can work as an actuator or micro-regulator (e.g. that can release insulin in response to changes in blood glucose levels). Biocatalyst based biofuel cells could offer better biocompatibility, but besides that, the BFCs life-time and biofouling problems must be taken into account [18]. Miniaturization of biofuel cells may allow full portability of the device which opens the opportunity for *in-situ* analysis both in the clinical and environmental fields [16].

BFCs can be applied to power up tiny components like Walkman devices, implantable medical devices (pacemakers [19], brain-machine interfaces [20], artificial organs [21]) and many other electronics like robots [22].

The development of biofuel cells for practical applications is a field that is still in its infancy, although there is unquestionably much potential for further improvement. Several areas present themselves as potential avenues for exploration. Implantable self-powered biosensors are one of the most active areas in the field owing to the ready availability of fuels such as glucose or lactate in living systems. The high turnover of enzymes can generate power levels capable of meeting the power demands of many devices, although methods of “wiring” the enzyme would be required to remove the need for a soluble mediator [16].

1.4. Brief History of Biofuel Cells

In the late 18th century, the first experiments were made that showed the possible connection between electricity and biological matter. It all began with the famous Luigi Galvani (Italian doctor, researcher, physicist, and philosopher) that made one of the first forays into the study

of bioelectricity, a field that still studies the electrical pattern and signals of the nervous system. Galvani, with the experiments on twitching of dissected frog legs after being bridged to the nerve through metal conductors, recognized the existence of an “animal electricity” as a vital force and organic movement as a bioelectric phenomenon. Years later, Alessandro Volta (Italian’s physicist) would contest the theory, arguing that electricity had dissimilar metal nature as the source. Alessandro Volta applied his work to later develop the first electric battery [23; 24].

The observation of biological activity as a possible source of electric energy was demonstrated by the botanist M.C Potter in 1911. In his study, electrical energy was produced from the fermentative process of *Saccharomyces cerevisiae* yeast cultures. The galvanic cell was implemented by immersion of platinum electrodes in a glucose-rich nutritive media. The addition of the yeast resulted in a gradual increase in voltage, close to 0.3 and 0.5 V. This galvanic cell was recognized as the first biofuel cell [25]. Years later were developed half cells of bacterial cultures connected in series which managed to obtain over 35 V [26].

In the ’60s, major advances in the bioelectrochemical energy have emerged. During those years, several biocells were developed emphasizing several potential applications such as in the identification of toxic materials, powering pacemakers and power suppliers in a remote area [27]. Preliminary experiments employing the enzyme glucose oxidase (GOx) as biocatalysts were reported in 1962 and their use was successfully accomplished ever since [28; 29]. The “enzyme electrode” term was first mentioned in 1967 [30].

More considerable advances were achieved during the ’70s, particularly the accomplishment of direct electron transfer (DET) between the catalytic center of immobilized redox proteins and the electrode surface. With this, the electroreduction of O_2 to H_2O_2 performed by an oxygen reduction enzyme was possible without the presence of a mediator compound. The achievement opened the possibility for further simplification of biofuel cell construction by eliminating the physical membrane that separates the anode and cathode compartments [31; 32].

Katz et al. developed in 1999 the first compartmentless enzymatic biofuel cell with both bioanode and biocathode presenting the DET feature. The power produced with this concept was low to be used as an energy supplier, about 4-5 $\mu W.cm^{-2}$ in a 1 mM glucose air-saturated buffer solution [33]. Biofuel cells with DET capability enabled the development of the concept “self-powered biosensor”, showing that the open-circuit potential of the system varied according to the fuel concentration and so, a calibration curve could be obtained [34].

In the early 21st century started the first experiments on biofuel cell operating *in vivo*. The first attempt was done by implanting a tiny biofuel cell in a grape, being able to produce about 240 $\mu W.cm^{-2}$ at 0.52 V [35]. In 2010 a biofuel cell was implanted successfully in a living animal, a rat without impeding normal activity and movements and producing 24 $\mu W.mL^{-1}$ at 0.13 V [36]. This experiment aimed at future medical prosthesis powered through enzymatic biocatalysts.

1.5. Enzyme Characteristics to be Used in Biosensors and Biofuel Cells

Enzymes are extensive, linear chains of amino acids or proteins (with 10-40 kDa) folded into three-dimensional compounds. They are important biomolecules and are accountable for all those inter-conversion processes which are needed to maintain life. Enzymes are biocatalyst, which means they are capable of accelerating a chemical reaction, by lowering the activation energy for chemical conversion of metabolites, without being part of the final product or being consumed in the process. To this, they are abundantly distributed in living beings in a great variety due to the very specific role each one is needed [37; 38].

Both enzyme and substrate have a particular complementary geometrical structure that fitted appropriately in one another, also called "the lock and key" model (Figure 4). This model is useful to explain the mechanism of action of enzymes that have strict specificity, but the model requires a level of rigidity that is incompatible with the current knowledge of molecular structure and conformation of macromolecules. Some agents cause conformational changes in enzymes. Another hypothesis is the "induced fit" model (Figure 4), which takes into consideration that the enzyme structure is adaptable [39].

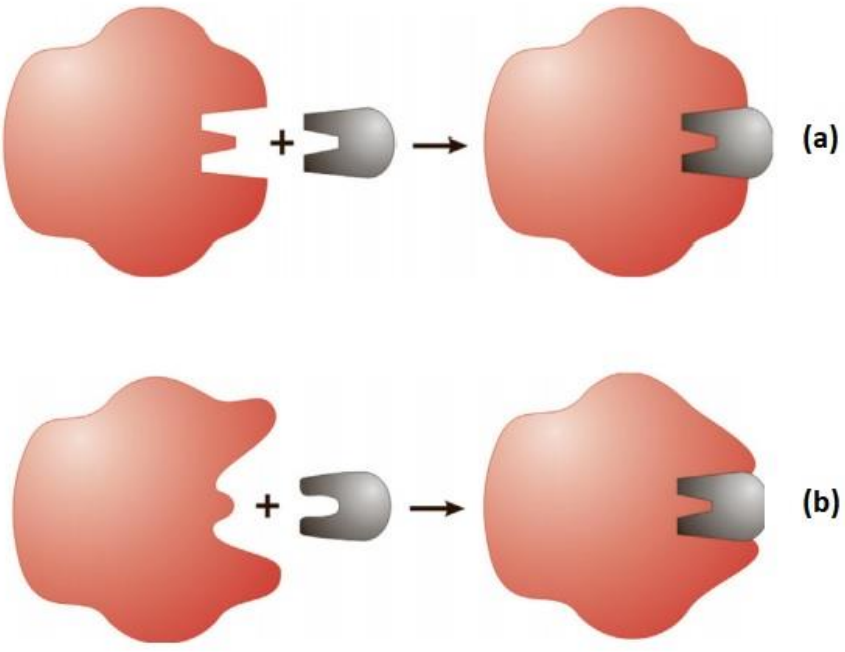

Figure 4- Representation of "lock and key" model (a) and "induced fit" model (b), adapted from [39].

Enzymes contain an active center that contains a catalytic residue that binds to a specific substrate and then completes the reaction. The active redox center can be composed of weakly bounds (eg. NADPH/$NADP^+$ or NADH/NAD^+ redox centers) or strong bounds. It can also be located near, peripheral, or deep in the protein or glycoprotein shell [12]. The active center may consist of metal-based cofactors (e.g. heme, iron-sulfur clusters, copper or copper-zinc), held through coordinate-covalent bonds on the amino acid side chains, inorganic ligands or prosthetic groups, while others enzymes make use of pure organic cofactors (e.g. flavin adenine dinucleotide, FAD, and pyrroloquinoline quinone, PQQ) [40].

Some enzymes also have bindings sites for tiny non-protein and thermostable molecules which can help to enhance or reduce the enzyme activity, working as a source of control [39]. The enzyme or complex enzyme-substrate can also be inhibited. The enzyme inhibition could be irreversible (where the change in the enzyme molecule is permanent) or reversible [41].

All these characteristics inherent to enzymes, especially their catalytic feature, makes enzymes to be an excellent choice for bioelectrodes construction and further use in biosensor and biofuel cells assembly. So analytes of interest that happens to be substrates of enzymes are most often directly oxidized or reduced by the enzyme providing a measurable signal. Yet, in some cases, enzymes enable conversion of non-electroactive substrates into electroactive species which can be then processed by the electrode surface [35]. Also, the inhibitory effect of some compounds on enzyme activity makes possible detection through the decrease of the signal with the proportional increase of inhibitor concentration.

The specificity of enzymes allows them to have high selectivity to distinguish among different substances and even between optical isomers of a compound. This simplifies the design of a fuel cell because fuel and oxidant need not be separated by an ionically conducting membrane, and they can be introduced as a mixture, that is, mixed reactant fuel cells are possible [42].

The enzymatic efficiency is dependable on operating conditions such as temperature and pH. Normally, optimal enzyme activity is achieved close to physiological conditions corresponding to a temperature around 37°C and a pH of 7 [37]. Therefore, the operation of biofuel cells in these conditions can be seen as a practical advantage when compared with traditional fuel cells, being possible their use in specific *in vivo* applications. Furthermore, operation at mild conditions is environmentally favorable.

There are two mechanisms explaining the electron transfer between enzymes and electrodes in biosensors and biofuel cells: direct electron transfer (DET) and mediated electron transfer (MET), as demonstrated in Figure 5. The DET mechanism occurs when an electrochemical signal related to the cofactor of the enzyme is detected or the catalytic reaction has occurred without the use of extra chemical substances (mediators). Commonly, chemical mediators increase the kinetics of electron transfer [43]. The achievement of heterogeneous DET enables practical and easier application of enzymes to biosensors and biofuel cells. The bioelectrode can operate in a potential window close to the enzyme potential avoiding thus possible interferences and the use of additional reagents working as mediators is unnecessary [40; 44].

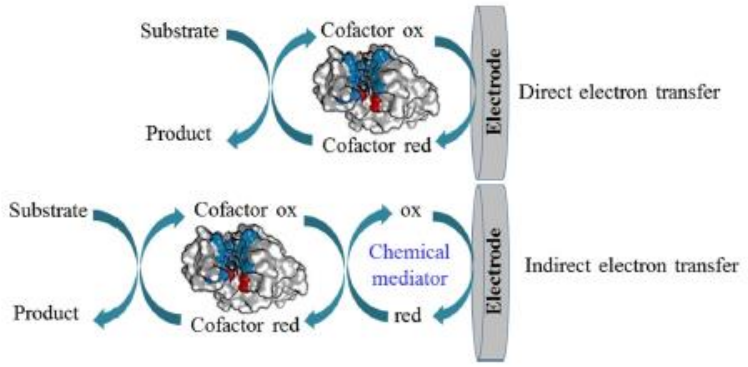

Figure 5- Direct and indirect electron transfer catalyzed by enzymes [43].

The establishment of DET is difficult and a challenging process and therefore the use of mediators is sometimes required. This is because the catalytic centers of enzymes are deeply buried in an insulating glycoproteic shell, acting thus as a barrier for electron transfer. The protein shell enclosing the active site protects it from hostile environments. Moreover, it has important functions since it defines the substrate selectivity and access, provides an internal electron relay system, proton access and the functional groups at the surface enable reactions for chemical attachment to other molecules or surfaces [42]. The catalytic properties of a given catalytic center can change depending on the proteinaceous environment where it is incorporated [40].

In the international enzyme classification, six major classes of enzymes are considered based on acting on the organic substrate, including the following [43; 45].

- ***Oxidoreductases***: Catalyze redox reactions;
- ***Transferases***: Enzymes that catalyze the transfer of a group of atoms, such as amine, carboxyl, carbonyl,(…), from a donor substrate to an acceptor compound;
- ***Hydrolases***: Enzymes that catalyze the hydrolysis of molecules;
- ***Lyases***: Catalyze the cleavage of C-C, C-O, C-S and C-N bonds (excluding peptide bonds) through adding a functional group to the molecule;
- ***Isomerases***: Catalyze the addition of a functional group to a molecule to form an isomeric of any type, for example, optical isomers, geometric isomers, and positional isomers;
- ***Ligases***: Enzymes that catalyze the coupling of two or more molecules.

Oxidoreductases, or redox enzymes, are the most attractive bioreceptor even in the commercial aspect [43]. Redox enzymes enable electron exchange to/from specific compounds along energy chains. They consist of a redox center assuring bioactivity embedded in a complex polypeptide tertiary structure conferring stable function in surrounding microenvironment and specifying a particular reacting compound, the substrate [38].

Redox enzymes are divided into five major categories (Figure 6). A number of different biosensors and biofuel cells can be implemented given the multiplicity of redox enzymes available. Moreover, isozymes derived from different organisms may present substantial differences regarding catalytic activity and redox potential offering therefore diverse options for optimized use in the intended application.

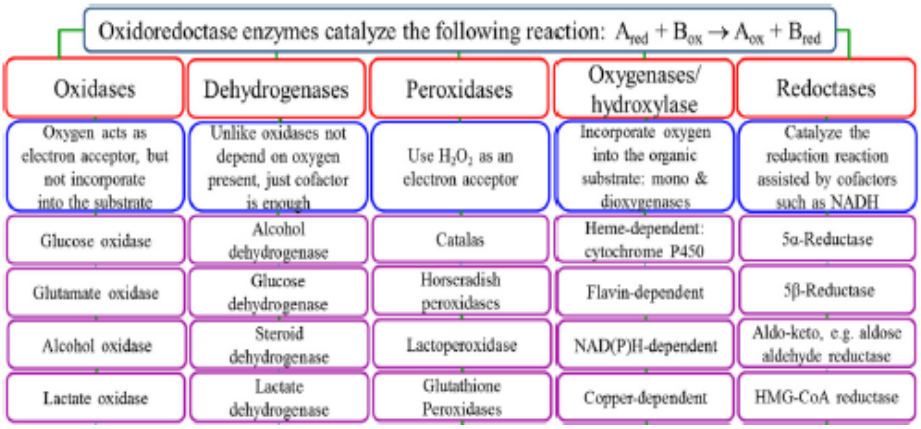

Figure 6- Oxidoreductases categories and subclasses based on their function, adapted from [43].

Normally, enzymes alone are inappropriate for been used for many aspects: commonly enzymes are soluble, repressed by substrates, products, and other components, with average stability and with no perfect catalytic properties. The enzyme immobilization brings a lot of characteristics like pH tolerance, performance in organic solvents, heat resistance, more flexibility, and more functional stability or selectivity. Some immobilized enzymes can also be used continuously before losing activity [46].

This work will be focus mainly on the most commonly used enzymes in biofuel cells, namely multicopper oxidases at cathodes and the flavin-containing GOx at the anode since these enzymes generally operate at physiological conditions and possess high activity. Their mechanism of action is well described in the literature [32; 40].

1.6.Strategies for Enzyme Immobilization

Enzyme immobilization has become an essential process in many industries over the last decade. Science has developed many emerging techniques of enzyme immobilization that allow the fabrication of biofuels, biosensors and the synthesis of the biocatalyst. Immobilization can be described as a technique that contains stabilizing of a biocatalyst in or on the insoluble matrix. Instability of enzymes often limits their usages in sensor devices. To produce enzyme-based electrochemical biosensors, enzymes should be immobilized on a solid surface (electrode) for efficient electron transfer [43].

The immobilization can be done through diverse methods, generally characterized as chemical and physical methods. Physical methods produce weak interactions between enzymes and the support while in chemical methods there is the establishment of covalent bonds. The progress

in organic chemistry and molecular biology had a direct impact on the evolution of immobilization technics [37].

In the construction of biosensors and biofuel cells, immobilization of the biological entity on the surface of the electrode has become common sense. This makes the system much simpler for various reasons. First, lower quantities of biocatalysts are needed when they are concentrated in the vicinity of the electrode instead when used soluble in the electrolyte. Second, bioelectrodes tend to be portable and reusable in different solutions. Third, the immobilization process may provide a friendlier environment for the biological entity, increasing, therefore, the stability and lifetime of the system. And lastly, and efficient immobilization may achieve a DET process increasing the system performance and simplicity. So, in order to obtain an efficient and/or durable system, the immobilization procedure must be carefully equated and tested since it is the most challenging and sensitive process in the construction of biosensors and biofuel cells [43].

There are numerous procedures for enzyme immobilization (Table 2). Many research papers and reviews have been published related to the enzyme immobilization techniques along with comparison, advantages, and disadvantages [47; 48]. Some strategies have been suggested based on the coupling of multiples immobilization methods [43].

Table 2- Conventional Enzyme Immobilization Techniques, based on [37].

Enzyme Immobilization Technique	Method Type	Description
Covalent Pairing	Chemical	A molecular bond that involves the sharing of electron pairs between atoms.
Adsorption	Physical or Chemical	Adhesion of atoms, ions or molecules from a gas, liquid or dissolved solid into a surface/matrix.
Ionic bonding	Chemical	Ionic interactions between enzyme with an opposing charge matrix.
Crosslinking	Chemical	Bonding enzymes through covalent pairing
Encapsulation	Physical	Enclosing enzymes in a semi-permeable membrane capsule.
Entrapment	Physical	Secure the enzyme in a porous structure
Complexation of chelation	Chemical	Enzymes are binding to a metal ion.

Adsorption, covalent bonding, entrapment/encapsulation and cross-linking (Figure 7) are the most common types of enzyme immobilization methods in the construction of biosensors and biofuel cells, which will be discussed in more detail.

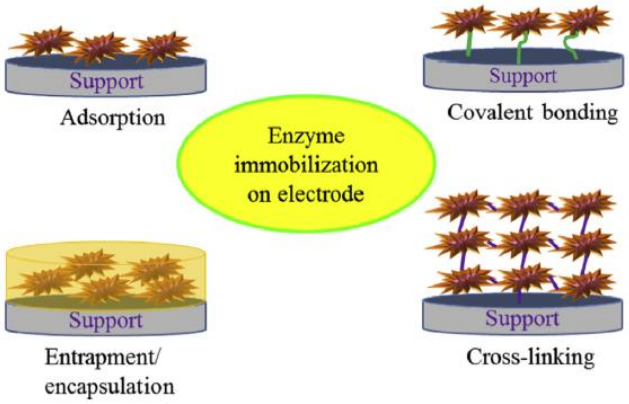

Figure 7- The most common types of enzyme immobilization techniques [43].

Adsorption is an old and easy process with extensive applications. This method is mainly based on the intramolecular forces, such as van der Waals, ionic, π-π or hydrogen bonding forces. This type of immobilization is usually reversible and the electrode is reusable [43]. The enzyme can be immobilized through simple mixing of the enzyme with an appropriate adsorbent under favorable conditions of temperature, pH and ionic power [37]. Carbon-based materials such as graphite, carbon nanotubes, and graphene along with noble metals, such as Au, Pt or Ag and metal oxide nanoparticles, are used as common conductive support. Generally, enzymes have different functional groups with a strong affinity to metal surfaces.

The electrode surface should be modified to achieve better enzyme loading and to improve efficiency. For example, the "layer-by-layer" stacking (Figure 8), in which the enzymes are sandwiched between two or more layers of conductive polyions with opposite charges (e.g. chitosan, polyethyleneimine, poly-butanylviologen; e.g) [43]. The modification of the enzyme orientation through primary functionalization can also improve the adsorption method, and for that, the hydrophobicity or hydrophilicity of the electrode surface shall be altered [38].

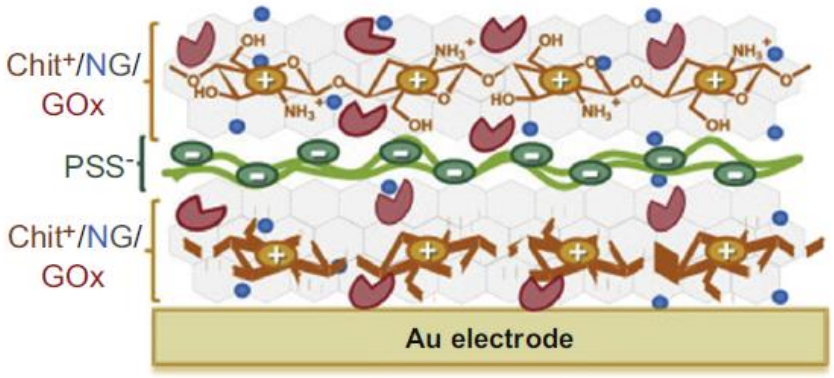

Figure 8- Layer-by-layer technique [49].

Covalent bonding involves the sharing of electron pairs between enzymes and the support matrix [37]. Several chemical compounds have been proposed for covalent immobilization. However, a few of them are applicable in bioelectrochemical approaches, because the chemical modifier may decrease the activity of the enzyme and hinder the electron transfer. Covalent bonding is usually irreversible and the electrode is not reusable [43]. The direct covalent linkage between enzyme and a matrix occur due to organosilanes or organic molecules containing -COOH, -NH_2, -SH, -OH terminal moieties, such as side-chain amino acids (e.g. aspartic acid), polypyrrole, indolyl, phenolic hydroxyl, and limidazole [37; 50; 51]. There are two main techniques for direct covalent immobilization that have been proposed decades ago and still being implemented with some modifications (Figure 9) [50].

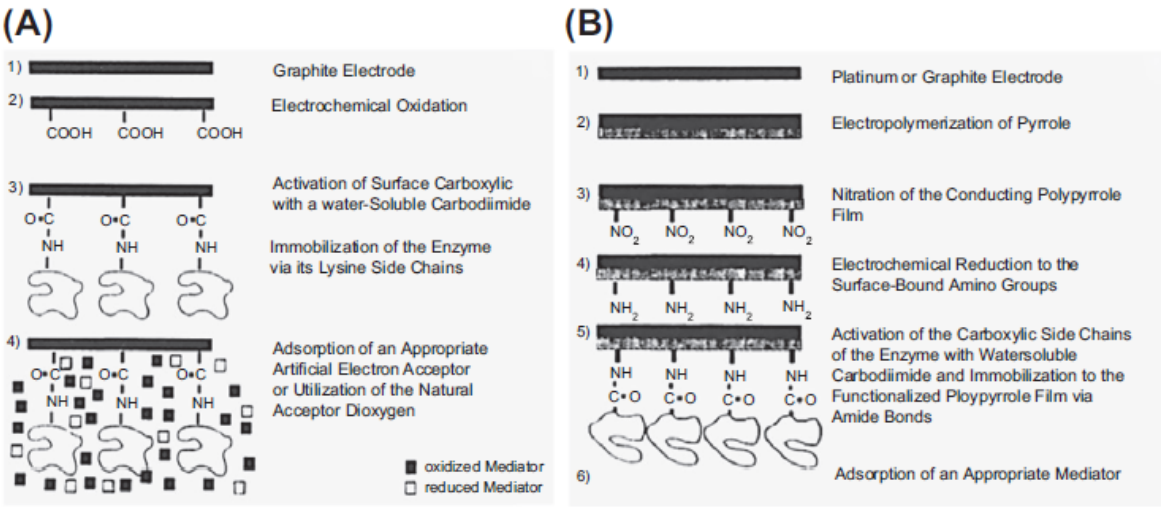

Figure 9- Direct Covalent Immobilization methods through electrochemical treatment to create carboxyl groups aimed at post-functionalization with an enzyme (A) and electropolymerization of pyrrole followed by electrochemical reduction and enzyme incubation (B) [50].

The first one consists in treating a carbon-based material like graphite, chemically or electrochemically, to generate the carboxyl groups. Those functional groups can be activated by EDC/NHS or DCC followed by enzyme incubation. The other method consists in a parallel way, such as polymerization of an organic compound containing a functional group on the surface of the electrode, followed by chemical or electrochemical treatment, activation and enzyme incubation.

Entrapment and encapsulation are techniques that can be expressed as the limited movement of enzymes in a matrix, however keeping them as a free molecule in the solution. On the entrapments process, the matrix has a porous structure with different sizes that can secure the enzyme in their network. In the case of encapsulation, the enzyme is enclosed in a semi-permeable membrane capsule, like hydrogels, conductive polymers and sol-gels [52]. Essentially, the enzyme is physically entrapped and stabilized in every direction within the polymer lattice. The matrix should have an efficient conductivity and must be permeable to the substrate and product to ensure continuous transformation. This method is simpler, produces stable biosensors and preserves the intrinsic properties of the enzyme for longer periods of time, but is impossible to control the enzyme orientation [43].

The crosslinking technique (Figure 10) includes the binding of biocatalyst via bifunctional or multifunctional ligands. This process consists of the bonding of enzymes between other enzymes, through covalent bonds. The bifunctional groups can be identical or nonidentical reactive groups. The most common bifunctional reagent used for enzyme immobilization is glutaraldehyde [43]. This method has some drawbacks such as hard experimental process, difficulties in the mass transfer of substrate and unwanted activity loss [37]. Like other methods, the electrode can be primarily modified to enhance immobilization, sensitivity, and stability [43].

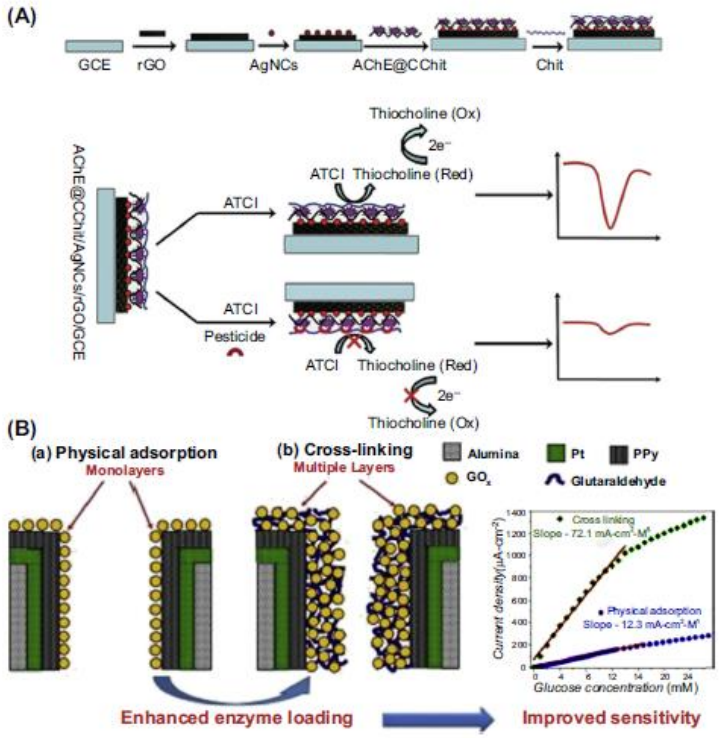

Figure 10- Two examples of enzyme cross-linking: Inhibition-based biosensor (A) [53]; GOx immobilized on polypyrrole nanotubes by glutaraldehyde (B) [54].

1.7.Glucose/O_2 Biofuel Cells

Glucose is the most universal building block in carbohydrates. It is also easily assimilated by most living cells and used as a source of energy or for the production of new cells [55]. Being a basic component of many other molecules, such as sucrose and lignin, glucose is extremely abundant in nature [56]. Glucose oxidase (GOx), as depicted in Figure 11, is an enzyme that breakdown glucose into gluconic acid in the presence of dissolved oxygen which acts as an electron acceptor, being reduced to hydrogen peroxide. Nowadays, GOx is commercially produced from *Aspergillus niger* and *Penicillium glaucum* through a solid-state fermentation method [57].

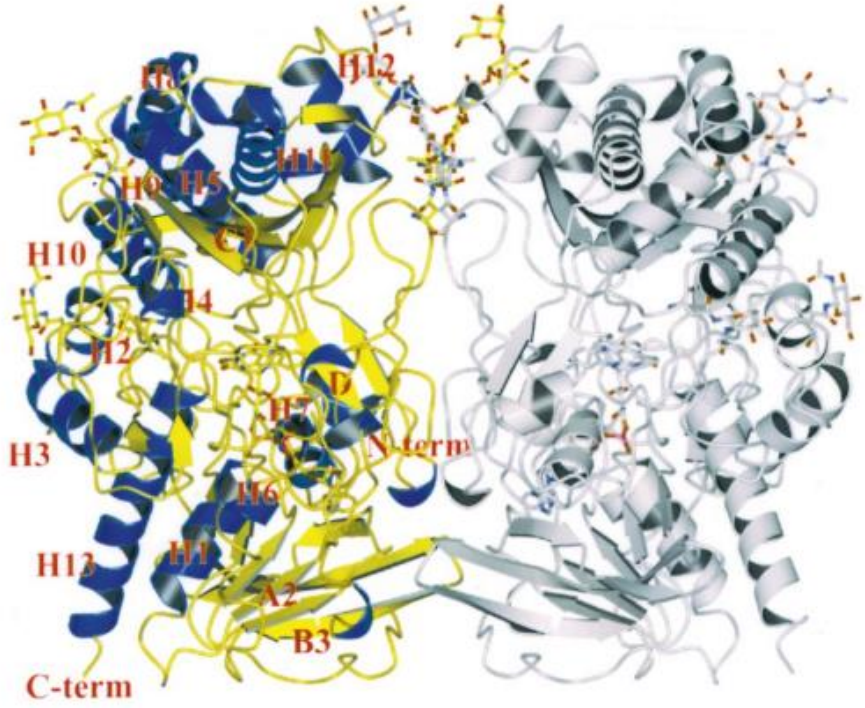

Figure 11- Ribbon diagram of glucose oxidase with the attached carbohydrate and the cofactor FAD [58].

GOx is a well-known and widely used redox enzyme in the electrochemical field due to the clinical importance of the glucose substrate as well as the commercial success of the glucose biosensor. This has led to intensive research on this molecule and to the development of innumerous biosensors for glucose determination and biofuel cells using glucose as fuel [59]. Since glucose is widely available in biological fluids, it can be potentially used to feed an implantable biofuel cell for powering valves, actuators or a pacemaker in the human body. Therefore glucose/O_2 biofuel cells have been studied as implantable devices [60]. In Table 3 are present some examples of developed glucose/O_2 biofuel cells with their respective composition and performance.

There are three different generations of glucose biosensors accordingly to the different mechanisms of glucose oxidation catalyzed by GOx (Figure 12).

On all of those mechanisms, FAD is the only cofactor for the catalysis reaction. The first generation is based on the electroactivity of the receptor substrate or the product. In a way, the electrode (traducer) may be sensitive to O_2 or H_2O concentration. In the second-generation sensor, there is present a chemical mediator to enhance the electron transfer (MET) to the electrode. Glucose is first oxidized by GOx and the generated electrons will reduce the mediator. The reduced form of the mediator is then oxidized at the electrode surface producing a measurable signal. The third generation is based on the DET mechanism. The electrons produced from the GOx catalysis are directly transferred to the electrode surface, without requiring oxygen or mediators [43].

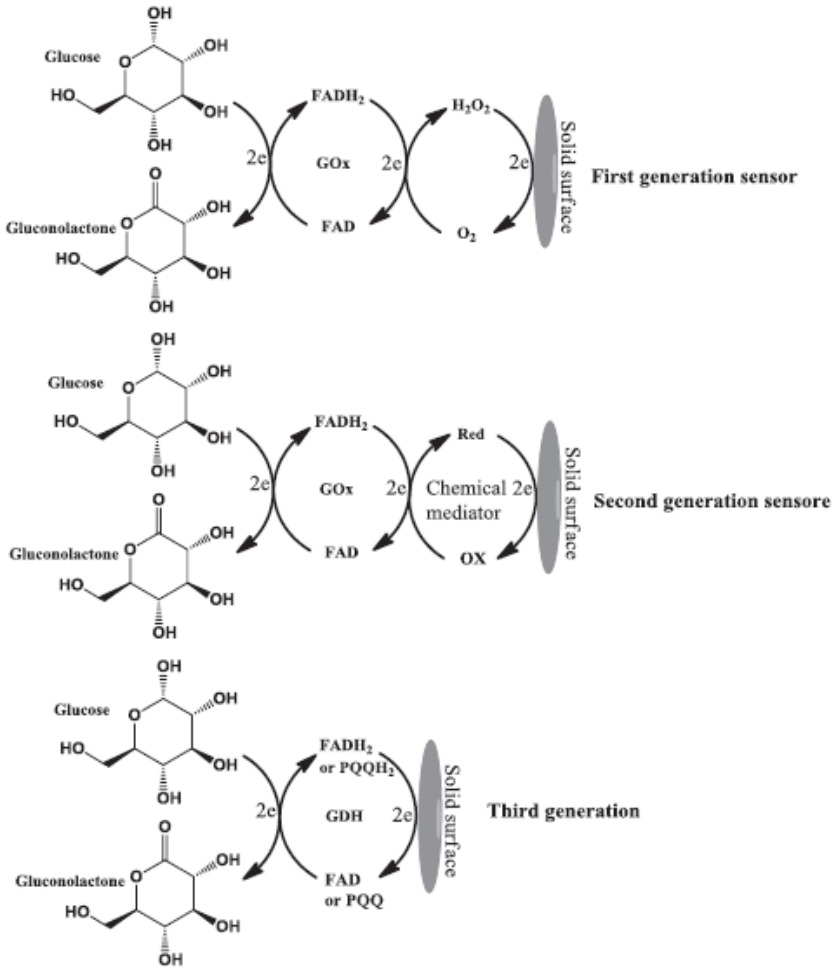

Figure 12- Different mechanisms of glucose oxidation reactions by GOx [43].

Different modified electrodes have been created in recent years for glucose/O_2 sensing, based on conductive polymer films or nanomaterials. Carbon-based nanomaterials and gold nanostructures are the first choices, for the fact that they have high conductivity, shown an enzyme-friendly environment, cost-effective and high surface area [43]. Recently, carbon nanotubes have attracted more attention aimed at GOx immobilization [61]. Some examples of glucose/O_2 biofuel cells are demonstrated in Table 3.

Table 3- Different types of glucose/O_2 biofuel cells.

Anode (Anolyte)	Cathode (Catholyte)	Separation membrane	OCP (V)	Power density ($\mu W.cm^{-2}$)	Reference
GCE/PAA-VK_3-diaphorase-PEGDGE/PLL-PEGDGE-GDH (10 mM glucose, 0.5 mM NADH, air sat., PBS pH 7)	Pt/PDMS (same as anolyte)	No	0.62	14.5	[62]
Carbon_Fiber/Os_polymer-PEGDGE-GOx (15 mM gluc., air sat., citrate pH 5)	Carbon_Fiber/Os_polymer-PEGDGE-laccase (same as anolyte)	No	-	110	[63]
Au/MWCNTs-PEG-TMOS-GOx (100 mM gluc., 4 mM ferrocene methanol, PBS pH 7.2)	Au/MWCNTs-PEG-TMOS-BOD (8 mM ABTS, O_2 sat., PBS pH 7.2)	Yes	0.48	120	[64]
PyrGE/SWCNTs/polyphenosafranin/GA-BSA-GDH (40 mM gluc., 10 mM NAD^+, PBS pH 6)	PyrGE/SWCNTs/MG/BSA-laccase (0.46 mM ABTS, PBS pH 6)	Yes	0.82	64	[65]
Buckypaper/PBSE/GDH (Implanted in lobster)	Buckypaper/PBSE/laccase (Implanted in lobster)	No	0.54	640	[19]
Aluminium-AuAgNPs/CB (5 mM gluc., KOH)	Aluminium-CB/ABTS/laccase (O_2 sat., PBS pH 5.0)	No	1.00	510	[66]
Glassy_carbon_Disck/Poly(4-vinylpyridine)/Os_polymer-sGDH (50 mM gluc., 3 mM $CaCl_2$, 30mM MOPS, air sat., PBS pH 7.0)	Glassy_carbon_Disck/Poly(4-vinylpyridine)/Os_polymer-Bromoethyl-amine-BOD (same as anolyte)	No	0.44	58	[67]
Graphene_SWCNTs/GOx/Gr/MWCNTs cogel (100 mM gluc., air sat., 1 M Nitric Acid, 0.1 M NaPhos pH 7.0)	Graphene_SWCNTs/BOD/Gr/MWCNTs cogel (same as anolyte)	No	0.61	190	[68]
Graphene_3D-GN/Nafion/GOx/Fc/GCE (10 mM gluc., air sat., Acetate buffer pH 5.0)	Graphene_3D-GN-PTCA-DA/Nafion/Lac/GCE (same as anolyte)	No	0.40	112	[69]

Label: GDH (glucose dehydrogenase); VK_3 (vitamin K3); PDMS (Polydimethylsiloxan); GCE (glassy carbon electrode); PEGDGE (Poly[ethylene-glycol]diglycidyl ether); MWCNTs (multiwall carbon nanotubes); ABTS (2,2'-azino-bis[3-ethylbenzothiazoline-6-sulfonic acid]); Lac (Laccase); Nafion (sulfonated tetrafluoroethylene based); GA (glutaraldehyde); BSA (bovine serum albumin); MG (methylene green); PyrGE (pyrolytic graphite);TMOS (tetramethoxy silane); BOD (bilirubin oxidase); MOPS (3-[N-morpholino]propanesulfonic acid).

Table 3 - Different types of glucose/O_2 biofuel cells (continuation).

Anode (Anolyte)	Cathode (Catholyte)	Separation membrane	OCP (V)	Power density ($\mu W.cm^{-2}$)	Reference
Glassy_carbon/Carbonized_PVP-$RPPy_{1600}$/NiF/GOx (50 mM gluc., air sat., SDS pH 5.0)	Glassy_carbon/Carbonized_PVP-RPPy/NiF/laccase (0.5 mM ABTS, air sat., B-R pH 5.0)	Yes	1.16	350	[70]
GOx/PPy/Fc (100 mM gluc., Acetate buffer pH 5.0)	Pt/C (air sat., Acetate buffer pH 5.0)	Yes	0.416	130	[71]
CNTs-Fc/SF-GOx/GCE (70 mM gluc., 0.1M PBS pH 7.0)	Pt/C (air sat., 200 mM Acetate buffer pH 4.4)	Yes	0.48	51	[72]
Carbon_Nanofiber(CNTs)/GOx/Fe_3O_4/Au_NPs (5 mM gluc., air sat., 100 mM PBS pH 7.4)	Carbon_Nanofiber/BOD/Fe_3O_4/Au_NPs (air sat., 100 mM PBS pH 7.4)	Yes	0.68	126	[73]
GOx/Gr/Au-rGO_NPs/NiF+FcCA (100 mM gluc., air sat., 100 mM PBS pH 5.0)	Laccase/Gr/Au_rGO_NPs/NiF (same as anolyte)	No	0.64	2840	[74]
Nafion/GOx/$PANI_{1600}$_CNTs/GCE (100 mM gluc., argon sat., 100 mM PBS pH 7.2)	Nafion/Laccase/$PANI_{1600}$_CNTs/GCE+ABTS (air sat., 200 mM B-R Buffer pH 3.0)	Yes	0.78	1120	[75]
GOx/catalase-compressed MWCNT disk (Implanted in rat)	Laccase-compressed MWCNT disk (same as anolyte)	No	0.57	190	[76]
Au/PQQ-GDH-PANi/MWCNT (5 mM gluc.; 1 mM $CaCl_2$, 5 mM MES Buffer pH 6.5)	Au/BOD-MWCNT (same as anolyte)	No	0.68	70	[77]
GOx-SWCNTs/PPY 3D Composite (1 mM gluc., 500 mM NaCl, PBS pH 6.5)	Tyrosinase-CNP/PPY composite (same as anolyte)	No	0.19	160	[78]
GOx/catalase-compressed/MWCNTs disk (50 mM gluc., air sat., 100 mM PBS pH 7.0)	Laccase-compressed/MWCNTs disk (same as anolyte)	No	0.95	1250	[79]
Cross-linked GOx clusters-MWCNTs/Nafion (200 mM gluc., air sat., PBS pH 7.0)	Pt/C/Nafion (air sat., PBS pH 7.0)	Yes	0.43	180	[80]

Label: GDH (glucose dehydrogenase); RPPY (rectangular polypyrrole tube); NiF (nickel foam); MWCNTs (multiwall carbon nanotubes); FC (Ferrocenecarboxaldehyde); SF (silk film); FcCA (ferrocenecarboxylic acid); ABTS (2,2'-azino-bis[3-ethylbenzothiazoline-6-sulfonic acid]); Lac (Laccase); Nafion (sulfonated tetrafluoroethylene based); BOD (bilirubin oxidase).

Table 3 - Different types of glucose/O_2 biofuel cells (continuation).

Anode (Anolyte)	Cathode (Catholyte)	Separation membrane	OCP (V)	Power density ($\mu W.cm^{-2}$)	Reference
GOx/Fc-Pd aerogel (50 mM gluc., air sat., 100 mM PBS pH 7.0)	BOD-Pd/Pt aerogel (same as anolyte)	No	0.40	20	[81]
MWCNTs/thionine/AuNPs/GDH (50 mM gluc., 10 mM NADH, air sat., N_2 sat.,100 mM PBS pH 6.0)	MWCNTs/PLL/laccase (same as anolyte)	No	0.70	330	[82]
vaCNT/PABMSA/PQQ-GDH (10 mM gluc., air sat., 100 mM CiP pH 7.0)	vaCNT/PQQ/BOD (same as anolyte)	No	0.80	120	[83]
PPY/SWCNTs/GOx (10 mM gluc. in 100 mM PBS pH 7.4)	PPY/laccase/ABTS (same as anolyte)	No	0.77	1390	[84]
GOx/PEDOT/MWCNTs/PVI-Os/PEGDGE (60 mM gluc., air sat., 20 mM PBS)	BOD/PEDOT/MWCNTs/PAA-PVI-Os/PEGDGE (same as anolyte)	No	0.70	2180	[85]
GOx-graphene/SWCNTs foam (1 mM gluc., N_2 sat., 200 mM sodium acetate and acetic acid buffer pH 5.0)	Laccase/ABTS-graphene/SWCNTs foam (0.5 mM ABTS ,O_2 sat., 200 mM sodium acetate and acetic acid buffer pH 5.0)	Yes	1.20	2270	[86]
GOx/catalase/NQ-compressed/MWCNTs disk (50 mM gluc., air and O_2 sat., PBS pH 7.0)	Laccase-compressed/MWCNTs disk (same as anolyte)	No	0.76	1540	[87]

Label: GDH (glucose dehydrogenase); PPY (polypyrrole tube); MWCNTs (multiwall carbon nanotubes); FC (Ferrocenecarboxaldehyde); ABTS (2,2'-azino-bis[3-ethylbenzothiazoline-6-sulfonic acid]); Lac (Laccase); BOD (bilirubin oxidase); PEGDGE (Poly[ethylene-glycol]diglycidyl ether); PEDOT (poly[3,4-ethylenedioxythiophene]); PABMSA (poly[3-aminobenzoic acid-co-2- methoxyaniline-5-sulfonic acid]); vaCNT (vertically aligned carbon nanotubes); PQQ (pyrroloquinoline quinone).

1.8.Objectives of the Study

The main objective of this thesis was the development of a membraneless enzymatic glucose/O_2 biofuel cell based on the immobilization of glucose oxidase and bilirubin oxidase onto pencil graphite transducers. The following specific objectives were performed:

- Electrochemical characterization of pencil graphite electrodes and comparison with other conventional electrodes;
- Development of bilirubin oxidase based biocathode and its characterization as a biosensor for O_2;
- Development of glucose oxidase based bioanode and its characterization as a biosensor for glucose;
- Assembly of the membraneless glucose/O_2 biofuel cell and assessment of the power produced.

2. Materials and Methods

In this chapter, all the strategies and methods put in the building and characterization of both biosensors and Biofuel Cells are described, along with their experimental conditions.

2.1.Reagents and Solutions

All reagents used were analytical grade. Ethanol absolute (CH3CH2OH), hydrochloric acid (HCl, 37%), potassium chloride (KCl), potassium hexacyanoferrate III (K3Fe[CN]6), potassium hexacyanoferrate II trihydrate (K4Fe[CN]6.H2O), Sodium Hydroxide (NaOH), sodium phosphate dibasic (Na2HPO4), sodium phosphate monobasic (NaH2PO4) and sulfuric acid (H2SO4), dimethylformamide (DMF, C3H7NO), sodium dodecyl sulfate (SDS, NaC12H25SO4), 1-pyrenebutanoic acid succinimidyl ester (PBSE, C24H19NO4) were acquired from Sigma-Aldrich (Germany). Alumina of 0.3 and 0.05 µm was acquired from Buehler (Switzerland).

Stock PBSE solution was prepared by dissolving the solid in DMF to achieve the concentration of 10 mM, divided in aliquots, and stored at -20°C until use.

All aqueous solutions were prepared with ultrapure water (Millipore Simplicity 185, resistivity of 18.2 MΩ.cm at 25°C). The used electrolyte was a 0.1 M of sodium phosphate buffer saline (PBS, pH 7.0), prepared according to DeAngelis table [88] using Na_2HPO_4 and NaH_2PO_4.

An equimolar (5 mM) aqueous solution of $K_4Fe[CN]_6.H_2O$ and $K_3Fe[CN]_6$ with 0.1 M KCl was prepared to assess and compare electrodes performance.

Carbon nanomaterials such as single-wall carbon nanotubes (SWCNTs) and multi-wall carbon nanotubes (MWCNTs) (both functionalized with carboxylic groups) and graphene oxide (GO, dispersion in water, 4 $mg.mL^{-1}$) were brought from Sigma-Aldrich (Germany). The stock solutions of carbon nanomaterials were made by dispersing the solid carbon nanomaterial in solvent (DMF or SDS or ultrapure water) to achieve the concentration of 1 $mg.mL^{-1}$ and stored at room temperature.

The enzymes glucose oxidase from *Aspergillus niger* (GOx) and bilirubin oxidase from *Myrothecium verrucaria* (BOx) were acquired from Sigma-Aldrich (Germany). Stock enzymatic solutions were made by dissolving the solid in 0.01 M PBS pH 7.

2.2.Instrumentation and Electrochemical Measurements

All electrochemical measurements were performed using a potentiostat/galvanostat Metrohm Autolab controlled with GPES v3.0 software.

A three-electrode electrochemical cell was used in all electrochemical characterizations, except in the biofuel cell assembly, using a platinum electrode and silver chloride electrode (Ag/AgCl, 3 M) as auxiliary and reference electrode respectively. A pencil graphite electrode (PGE) was used as the main working electrode throughout the entire work. For comparison purposes, a pyrolitic graphite electrode (GP) 3 mm diameter, a glassy carbon electrode (GC) 3 mm diameter, boron-doped diamond electrode (BDDE) 3 mm diameter, screen-printed carbon electrode (SPCE) 4 mm diameter and a screen-printed gold electrode (SPAuE) 1.6 mm diameter were also tested as working electrode. Before use, GP and GC were mechanically polished with alumina abrasives of 0.3 and 0.05 µm using a polishing cloth and then ultrasonically cleaned in ethanol absolute for 2 min and rinsed with water. The diamond electrode was pre-treated electrochemically with a 2-step chronoamperometry method at -3 V and +3 V for 45 seconds each in sulfuric acid 0.5 M. Cyclic voltammetry analysis was performed as a comparison technique between electrodes or to assess enzymatic catalysis of the substrate in biosensors. Chronoamperometry was applied for analytical determinations of enzyme substrates (glucose and O_2) and subsequent construction of respective calibration curves. A volume of 10 mL was added to the electrochemical cell in all of these experiments.

Buffer solutions were prepared using pH-meter Crison micro pH 2002. An equimolar 5 mM potassium hexacyanoferrate [$Fe(CN)_6^{3-/4-}$] solution in 0.1 M KCl was used as an electrolyte for the characterization of sensors without immobilized enzyme, while 0.1 M PBS was used as an electrolyte for the characterizations of each biosensor and biofuel cell. In experiments requiring the absence of O_2, the electrolyte was purged with N_2 for 15 min. This is a common method for dissolved oxygen removal which is quick and effective [89; 90].

In the biofuel cell assembly, a two-electrode setup was used: biocathode and bioanode. Linear sweep voltammetry (LSV) was used for the determination of polarization curves and subsequent determination of power curves. The electrolyte used for biofuel cell experiments was composed of 0.1 M PBS pH 7 within the absence and presence of fuel and oxidant (glucose and O_2, respectively) and in absence and presence of the GOx enzyme mediator, 2 mM benzoquinone.

2.3.Bioelectrodes Preparation for Biosensors and Biofuel Cell

The PGE used as transducer for modifications and enzyme immobilization was fabricated using commercial pencil mines (BIC, 2 mm diameter) that were put in contact with the inner copper wire of shielded coaxial cables and isolated with heat-shrinkable sleeves. A transversal cut exposed the pristine PGE surface, which was mechanically polished with sandpaper P1000 followed by filter paper to smooth the surface. Alumina polishing was then performed using 0.3 and 0.05 µm suspended particles and cleaned by immersing in ethanol and subjected to ultrasound for 2 min and finally rinsed with water. The active surface of the electrode corresponded to 0.0314 cm^2, which was used for calculations of current densities.

Preparation of the bioelectrode for O_2 biosensor and biocathode: In order to increase the electron transfer efficiency of PGE, the surface was nanostructured with carbon

nanomaterials. First, a reduced graphene oxide (rGO) layer was formed in the PGE surface by depositing 7 µl of GO, left to dry at room temperature and reduced electrochemically by cyclic voltammetry along 50 scans within -1.2 V and 0.8 V at 50 $mV.s^{-1}$ in 0.1 M Na_2SO_4. The nanostructuration of the PGE was performed by depositing 2 aliquots of 3 µl of MWCNTs suspension (1 $mg.mL^{-1}$ in DMF) in the PGE-rGO surface and dried under an IR Lamp. The modified electrode was then immersed in the cross-linker solution (10 mM PBSE in DMF) for 1 h and further washed for a few seconds by immersion in 0.01 M PBS (pH 7.0). In this way, the pyrenyl moiety of each PBSE molecule has enabled the formation of an irreversible π-π stacking at its interface with the aromatic-like walls of the carbon nanomaterials [91]. The succinimidyl leaving group allowed the formation of a covalent amide bond after reaction between the terminal carboxyl with an amine group of the enzyme polypeptide chain [92]. The final step consisted of the immobilization of the enzyme. This was accomplished by immersing the electrode in 0.5 $mg.mL^{-1}$ BOx solution (prepared in 0.01 M PBS pH 7) for 90 minutes. The unbound enzyme was removed from the electrode surface by immersing in the electrolyte solution (0.1 M PBS pH 7) prior to the analysis. This bioelectrode is henceforth designated as PGE-rGO-MWCNTs-PBSE-BOx.

Preparation of bioelectrode for glucose biosensor and bioanode: The bioelectrode for glucose was prepared similarly as the BOx bioelectrode. In this case, SWCNTs were used instead of MWCNTs. Therefore, 2 aliquots of 3 µl of SWCNTs suspension (1$mg.mL^{-1}$ in DMF) were deposited in the surface of the PGE-rGO and left to dry under the lamp. This electrode was then immersed in the PBSE solution for 1 h and washed in buffer solution. Specifically for the immobilization of GOx, the modified electrode was immersed in the enzyme solution (10 $mg.mL^{-1}$ prepared in 0.01 M PBS pH 7) and left overnight at 4 °C for proper cross-linking. The bioelectrode was then washed in electrolyte prior to analysis. This bioelectrode is henceforth designated by PGE-rGO-SWCNTs-PBSE-GOx.

3. Results and Discussion

The main objective of this work was to develop a Glucose/O_2 Biofuel Cell system composed of bioanode and biocathode, based respectively on the enzymes glucose oxidase (GOx) and bilirubin oxidase (BOD). The experimental work began with the characterization and comparison of different transducers. Then, the bioanode and biocathode were individually studied as biosensors towards the respective enzyme substrates. Finally, the biofuel cell was assembled and its performance was assessed.

3.1.Electrochemical Characterization of Different Electrodes

The first stage of this work was to observe the effect of the different types of transducers by cyclic voltammetry in the presence of an equimolar mixture of hexacyanoferrate [$Fe(CN)_6^{3-/4-}$], performed at room temperature. In this chapter, many distinct transducer materials were studied, as well as the outcome of diverse dispersion agents and carbon nanomaterial modifications.

3.1.1. Electrode Pre-Treatment and Comparison of Unmodified Electrodes

Different types of unmodified electrodes materials such as GC, GP, PGE, BDDE, SPCE and SPAuE were studied regarding their electrochemical performance. The PGE electrodes were homemade while the other electrodes were commercially acquired and available in the laboratory.

Since the surface pre-treatment of the electrodes may significantly affect their performance, each electrode, except for the screen-printed, was subjected to a polishing treatment with alumina abrasives of 0.3 µm and 0.05 µm and thereafter subjecting them to ultrasound (2 min) in ethanol. This polishing procedures with alumina have been stated to improve the kinetics of the electrode in [$Fe(CN)_6^{3-/4-}$] [93] by affecting the microstructure and roughness of the surface [94] or by increasing the oxygen functionalities at the surface and thus its reactiveness to certain species [95].

Other articles have also confirmed an improvement in the electrotransfer system upon the pre-treated electrode when compared to the bare one [96; 97].

In Figure 13, a cyclic voltammogram of the tested PGE electrode with and without pre-treatment is represented.

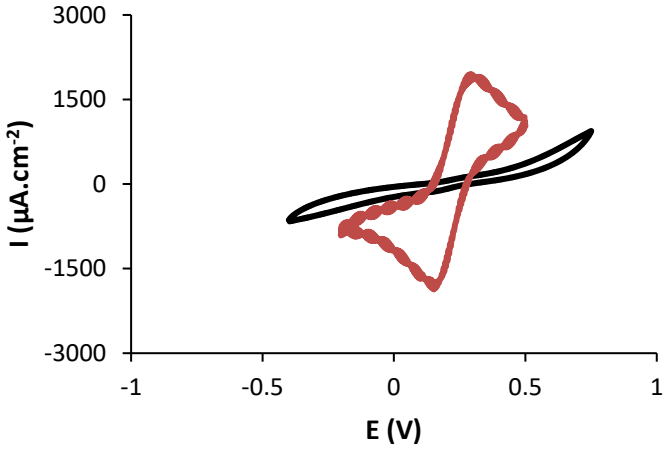

Figure 13- Cyclic voltammogram of untreated PGE (—) and pre-treated PGE with albumin (—) in hexacyanoferrate. Electrolyte: 5 mM $Fe(CN)_6^{4-}/Fe(CN)_6^{3-}$ with 0.1 M KCl. Scan rate: 100 $mV.s^{-1}$.

With these results, it was possible to conclude that the alumina polishing allows a general improvement of the electron transfer kinetics of the electrode by achieving defined voltammetric peaks.

The study about the behavior of different unmodified electrodes was carried on, with cyclic voltammograms of the redox system for each type of electrode being represented in Figure 14. Analytical data obtained from these voltammograms are also shown in Table 4.

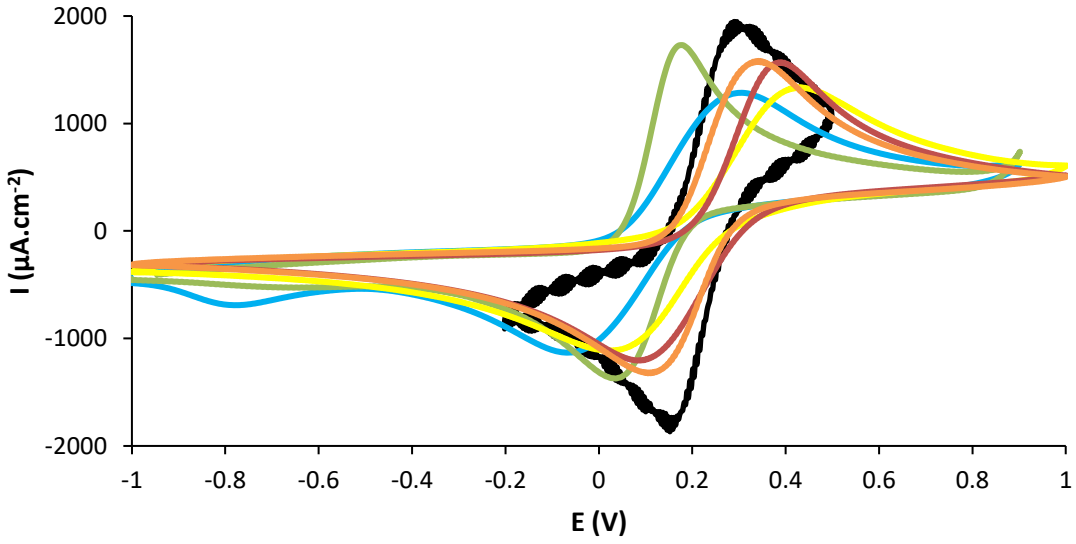

Figure 14- Cyclic voltammogram of pre-treated GC (—), GP (—), BDDE (—), PGE (—) and untreated SPCE (—) and SPAuE (—), in hexacyanoferrate. Electrolyte: 5 mM $Fe(CN)_6^{3-/4-}$ with 0.1 M KCl. Scan rate: 100 $mV.s^{-1}$.

Table 4- Peak currents, $|I_{p.red}/I_{p,oxi}|$, K^0 and ΔE_P of different biosensors materials.

Electrode type	GC	BDDE	GP	PGE	SPCE	SPAuE
	Pre-treated	Pre-treated	Pre-treated	Pre-treated	Non-treated	Non-treated
$I_{p,oxi}$ ($\mu A.cm^{-2}$)	1379	1655	1669	1671	1305	1850
$I_{p,red}$ ($\mu A.cm^{-2}$)	-1289	-1443	-1443	-1537	-1218	-1442
$\lvert I_{p.red}/I_{p,oxi} \rvert$	0.93	0.87	0.86	0.92	0.93	0.78
ΔE_P (V)	0.345	0.226	0.159	0.125	0.332	0.146
K^0 ($cm.s^{-1}$)	2.85E-04	8.28E-04	1.95E-03	3.04E-03	3.22E-04	2.12E-03

The cathodic/anodic peak current ratios ($I_{p.red}/I_{p,oxi}$) were closer to 1 for all benchmark redox systems. The ΔE_p obtained were all greater than 57 mV (expected for Nernstian one-electron reaction) which could indicate problems on the heterogeneous electronic transference probably due to a negatively charged nature of the working electrode surface [98].

Of all electrodes examined, the PGE electrode exhibited the most reversible behavior towards the redox couple by achieving lower ΔE_p, while GC and SPCE electrodes yielded the poorest reversibility and low current peaks values, probably due to the resistive properties that may have become a significant limiting factor [99].

The electrochemical performance of the electrodes measured through the evaluation of the heterogeneous electron transfer rate constant (K^0) was calculated based on the method of Nicholson [100] (Equation 1).

$$Eq\ 1: \quad k^0 = \Phi \left(D_0 \times \pi \times v \times \frac{n \times F}{R \times T} \right)^{0,5} \times \left(\frac{D_R}{D_0} \right)^{\frac{\alpha}{2}}$$

where Φ refers to a kinetic parameter, D_0 is the diffusion coefficient for the ferricyanide ($7.6x10^{-6}$ $cm^2.s^{-1}$), D_R is the diffusion coefficient for the ferrocyanide ($6.3x10^{-6}$ $cm^2.s^{-1}$), α is the transfer coefficient (0.5), R is the universal gas constant (8.314 $J.K.mol^{-1}$), T is the absolute temperature (at room temperature, 298 K), n is the number of electrons transferred (n=1 for the $Fe(CN)_6^{3-/4-}$redox system), π is the pi number (≈3.14), v is the scan rate (0.1 $V.s^{-1}$) and F is the Faraday constant (96 485 C).

The kinetic parameter (Φ) varies with the peak potential separations (ΔE_p) and this relation can be observed in Figure 15.

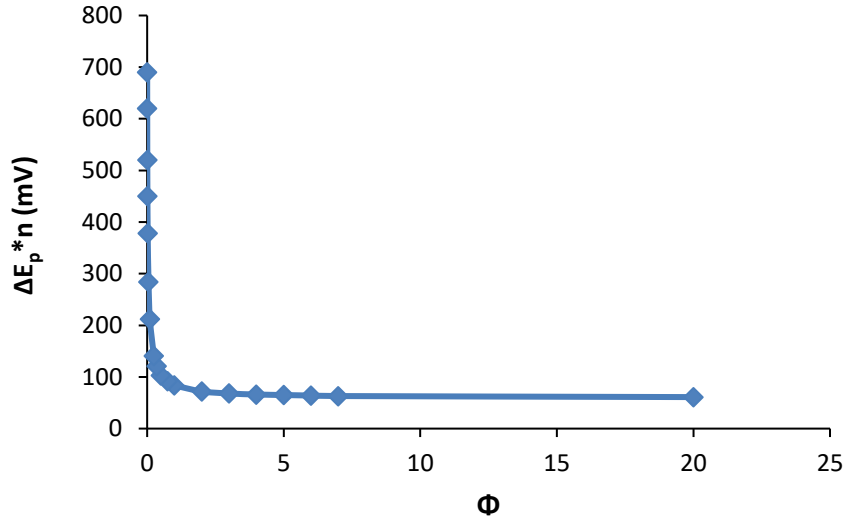

Figure 15- Variation of peak potential with kinetic parameters for cyclic voltammetry, adapted from [100; 101].

According to the K_0 results obtained, the electrodes charge-transfer mechanics can be described as quasi-reversible, by the fact that $0.3x[v.n]^{0.5} > K_0 > 2x10^{-5}*[v.n]^{0.5}$ [101].

Since the PGE electrode was the only one that was constructed in the laboratory, its results will heavily depend on the way it is built and treated. Besides that, the results obtained for polished PGE were better in contrast to the other electrode types. PGE is a cheap and very reliable material, being a good choice as a substrate for modification and enzyme immobilization in the development of biofuel cell systems.

3.1.2. Comparison of Different Carbon Nanomaterials Modifications on the PGE Electrode Surface.

The modification of the PGE surface with different carbon nanomaterials, namely MWCNTs, SWCNTs and rGO was studied and compared.

The level of carbon nanomaterial dispersion in the solvent is important and affects the electrochemical response. So, the dispersion of carbon nanomaterial in three different media was first assessed by modifying the pre-treated PGE with MWCNTs suspension in dimethylformamide (DMF), water, and the anionic surfactant SDS (Figure 16).

The electrochemical parameters obtained from the CVs different modifications are shown in Table 5.

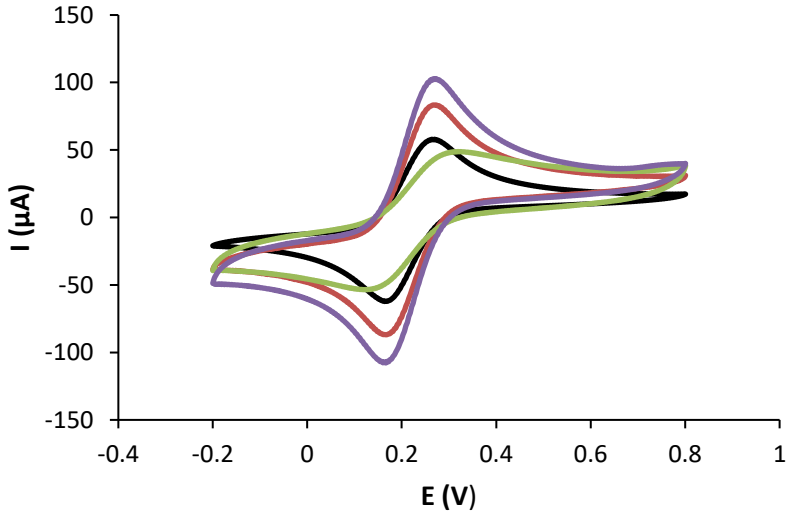

Figure 16- Cyclic Voltammograms of bare PGE electrode (—) and PGE modified with MWCNTs dispersed in different media: DMF (—), Water (—) and SDS (—). Electrolyte: 5 mM $Fe(CN)_6^{3-/4-}$ with 0.1 M KCl. Scan rate: 100 $mV.s^{-1}$.

Table 5- Anodic and cathodic potential peaks for the different PGE electrode modifications strategies.

PGE Modification	$I_{p,oxi}$ (µA)	$I_{p,red}$ (µA)	$\lvert I_{p.red}/I_{p,oxi} \rvert$	ΔE_P (V)
Bare PGE	66.4	-64.9	0.98	0.095
PGE-MWCNTs (Water)	88.5	-90.9	1.03	0.092
PGE-MWCNTs (DMF)	102.0	-111.9	1.10	0.092
PGE-MWCNTs (SDS)	45.1	-45.0	1.00	0.152

Generally, the electrode modification with carbon nanomaterials tends to increase the electron transfer rate and the current peak due to the greater surface area [102].Particularly, MWCNTs is widely used because it exhibits high sensitivity and low detection limits [103]. According to the results in Table 5, the dispersion of MWCNTs in water or DMF shows a significant current increase of about 37% and 65% respectively when compared to the bare electrode. Moreover, the ΔE_p obtained in those were slightly better compared to the bare PGE electrode (≈-3%), which indicates a quasi-reversible behavior.

DMF is a common organic solvent which contains amide groups that can interact well with carbon nanotubes particles, enhancing the dispensability of the particles and the performance of the modified electrode [104].Water as a solvent for the MWCNTs also showed good results, however, without either chemical or non-covalent functionalization a good dispersion of carbon nanotubes couldn't be achieved [105].

SDS as a dispersing agent for MWCNTs showed the worst results, about -31% in current values and +58% in ΔE_p, when compared to the bare electrode. Although these results, some authors confirm that SDS can be used as a dispersing agent for carbon nanomaterials when functionalized with carboxylic groups [106; 107].

Considering the results obtained, it can be concluded that the best electrochemical response is obtained when the carbon nanoparticles are dispersed in DMF and therefore used as dispersing media for carbon nanotubes in modifications of PGEs hereafter while graphene was maintained in water due to well dispersion and high stability.

The modification of the PGE surface with different carbon nanomaterials was carried on next. In Figure 17, the different responses for the bare and modified electrode are presented. The electrochemical parameters obtained from the CVs of each modified PGE are shown in Table 6.

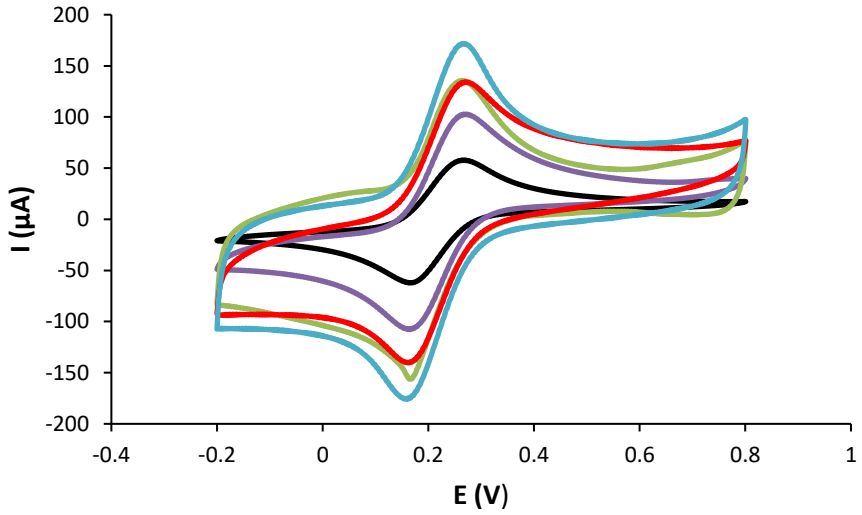

Figure 17- Cyclic Voltammograms of bare PGE (—) and modified PGE electrode: rGO (—), MWCNTs (—), SWCNTs (—) and rGO-MWCNTs (—). Electrolyte: 5 mM $Fe(CN)_6^{3-/4-}$ with 0.1 M KCl. Scan rate: 100 $mV.s^{-1}$

Table 6- Anodic and cathodic potential peaks for the different PGE electrode modifications strategies.

PGE Modification	$I_{p,oxi}$ (µA)	$I_{p,red}$ (µA)	$\lvert I_{p.red}/I_{p,oxi} \rvert$	ΔE_P (V)
Bare	66.4	-64.9	0.98	0.095
PGE-MWCNTs	102.0	-111.9	1.10	0.092
PGE-SWCNTs	91.6	-147.7	1.61	0.104
PGE-rGO	109.0	-116.7	1.07	0.104
PGE-rGO-MWCNTs	136.8	-151.9	1.11	0.101

According to Table 6, the values of ΔEp are close to 0.1 V for all PGE modifications, with a quasi-reversible behavior. Compared to the bare electrode, the reversibility of the modified electrode varies between -3% and +9%.

The carbon nanomaterials in the study (Figure 18) present different performance as results of their structure and form. Carbon nanotubes (CNTs) are seamless cylinders of one layer (SWCNTs) or multiple layers (MWCNTs) of graphene and they have high conductivity and high aspect ratio which help them to form a network of conductive tubes [108; 109; 110].

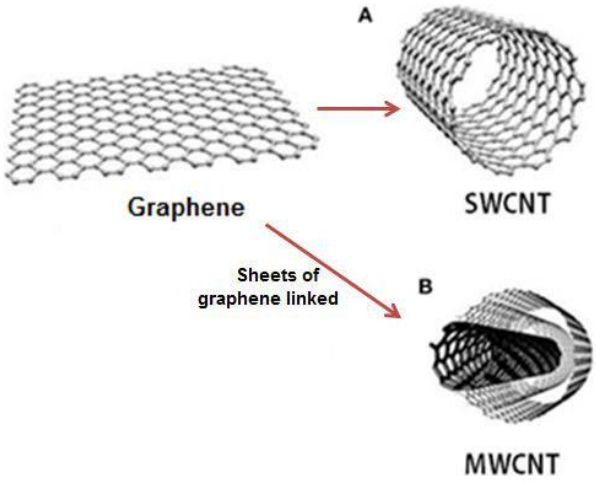

Figure 18- Structure representation of Graphene, SWCNTs and MWCNTs [111].

The modification with SWCNTs achieved an average current peak value 84% higher than the bare electrode, however, their current ratio value of 1.61 possible indicates weak electrochemical stability. SWCNTs have generally greater electrical conductivity with a metallic or semiconducting behavior depending on the roll orientation of the graphene sheet [110].

The modification with MWCNTs achieved an average current peak value of 65% higher than the bare electrode. The redox peaks are more well-defined and the current ratio is closer to 1. Besides their structural complexity and variety, MWCNTs have better chemical and mechanical stability, which are easier to produce and cheaper when compared to the SWCNTs [112; 113].

The PGE modified with rGO achieved an average current peak value of 74% higher than the bare electrode. The performance of PGE-rGO was similar to the PGE-SWCNTs, although their redox couple isn't so well defined, presenting also higher current capacity. Some authors end up choosing rGO over the CNTs because of the wide surface area and the roughness and wrinkled texture of the planer sheet structure that may be useful to strengthen the nanocomposites [114].

The double-layer modification on PGE with rGO and MWCNTs achieved an average current peak value of 124% higher than the bare electrode. The significant increase in the conductivity of the double-layer modification compared to the single-layer modification may be due to the synergy effect of the two nanomaterials by increasing the interlayer spacing and the effective surface area between the rGO and CNTs nanocomposite film [115].

Considering the results obtained, it can be concluded that all modifications applied promoted a better electrochemical response of the electrode. The best electrochemical response is obtained with a double-layer modification on the PGE electrode and therefore this type of configuration was considered for subsequent immobilization of enzymes. The compatibility and the level of dispersion between different carbon nanomaterials and the enzymes are relevant factors that may alter the electrochemical performance on the biosensor.

3.2. Characterization of GOx and BOx Bioelectrodes Used as Biosensors

The second stage of this work consisted of the fabrication of enzymatic bioelectrodes to be ultimately used as bioanode and biocathode in biofuel cells. Both bioanode and biocathode were first individually studied as biosensors towards respective enzyme substrates (glucose and O_2). Initially, CV analysis was performed to verify the electrochemical behavior of each substrate followed by their detection through an amperometric technique.

3.2.1. Characterization of BOx Bioelectrodes Used as a Biosensor for O_2 Detection

In order to assess the best enzymatic performance, different bioelectrodes configurations were compared by CV in the presence and absence of BOx substrate, O_2, dissolved on the electrolyte (Figure 19). The immobilization of BOx to the electrode was effectively achieved through the cross-linker 1-pyrenebutanoic acid succinimidyl ester (PBSE) enabling direct electron transfer (DET) and thus avoiding the use of a mediator.

Some articles confirm that the reduction of oxygen tends to affect the cyclic voltammograms between 0 to 2 V (corresponding to the region of oxygen absorption), shifting it to more negative currents [87; 116].

It can be observed that in the sensor without immobilized BOx (PGE-rGO-MWCNTs-PBSE) there was no difference between the CV curves with and without O_2 (Figure 19a) indicating that oxygen catalysis did not occur. Whereas in Figures 19b and 19d corresponding to bioelectrodes PGE-PBSE-BOx and PGE-rGO-PBSE-BOx respectively, the tendency of the CV curve in the presence of O_2 towards more negative values of current was minimum compared to the curve in absence of O_2 indicating poor efficiency of BOx enzyme in the reduction of O_2. This is probably due to the absence of functional groups in the graphite of PGE and rGO surface leading to a poor cross-linking of the enzyme to these carbon structures. On the contrary, the difference in the curves was more pronounced for bioelectrodes PGE-MWCNTs-PBSE-BOx (Figure 19c) and PGE-rGO-MWCNTs-PBSE-BOX (Figure 19e), especially for this last-mentioned bioelectrode, confirming good bioelectrocatalysis of O_2 from BOx.

Therefore, PGE modified with rGO-MWCNTs-PBSE-BOx is the most effective one, by the fact that the current capacity is bigger and the current shifting is more salient towards more negative current values (max. +3.3 µA). Also, this biosensor seems to be more sensitive to the presence of dissolved O_2 when compared to the double-layer with SWCNTs (Figure 19f).

So, PGE-rGO-MWCNTs-PBSE-BOx bioelectrode was selected for the amperometric detection of O_2 studies.

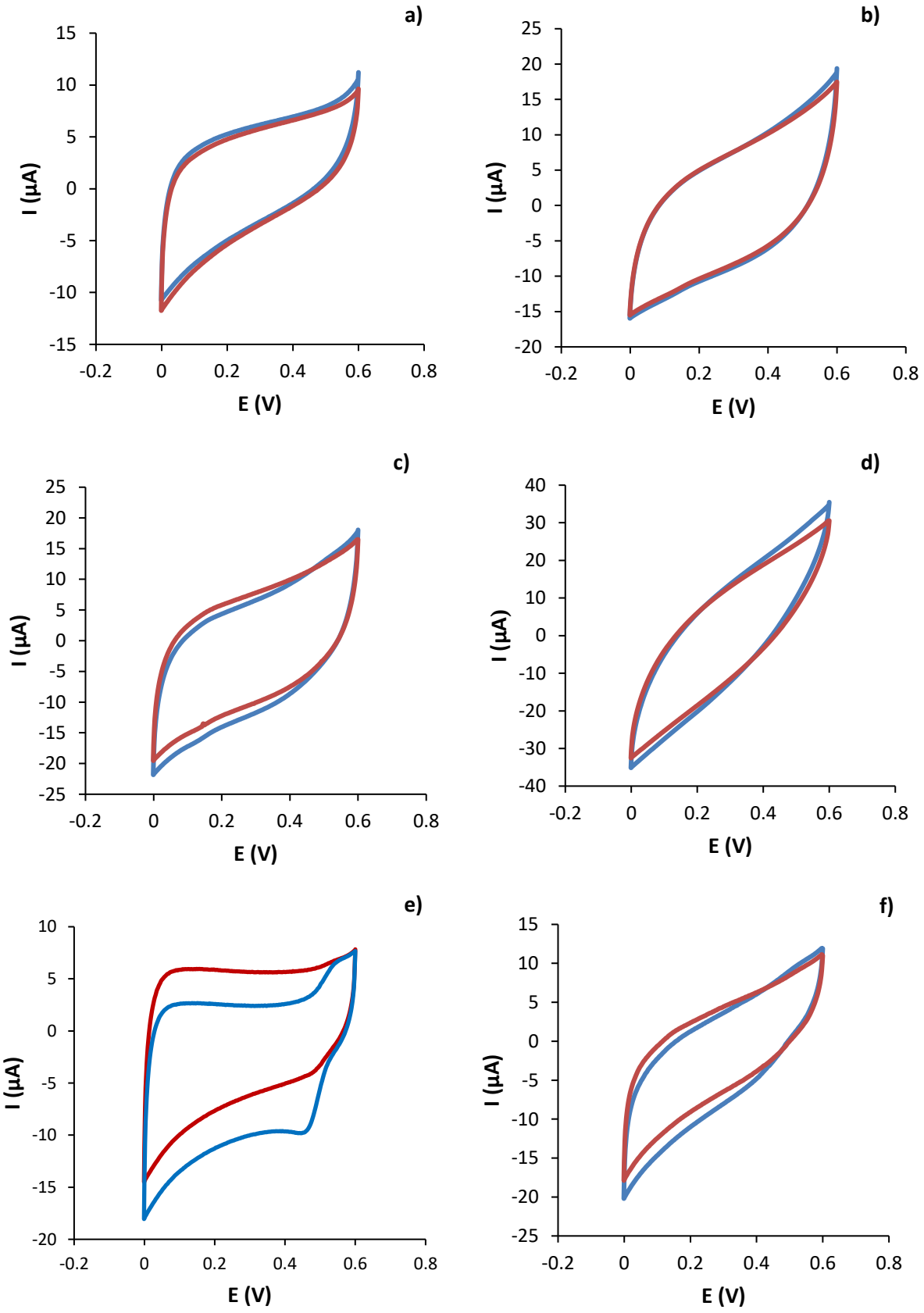

Figure 19- Cyclic voltammograms of the various configurations of electrode and bioelectrodes in the absence of O_2 (━) and presence of O_2 (━); Electrodes Modification: a) PGE-rGO-MWCNTs-PBSE, b) PGE-PBSE-BOx, c) PGE-MWCNTs-PBSE-BOx, d) PGE-rGO-PBSE-BOx, e) PGE-rGO-MWCNTs-PBSE-BOx, f) PGE-rGO-SWCNTs-PBSE-BOx; Electrolyte: 0.1 M PBS pH 7; Scan rate: 20 $mV.s^{-1}$.

The amperometric method is based on the measurement of current produced in an electrochemical cell at an appropriate applied voltage. The concentration of the species dissolved in the cell is proportional to the diffusion current [117]. In this study, a potential of +0.1 V was chosen to guarantee the proper electroreduction of O_2 from BOx as observable in Figure 19f. Various aliquots of buffer containing air and thus O_2 in a 21% relation were added to the electrochemical cell containing previously 10 mL of the buffer without O_2 (purged with N_2) and the current was measured when stabilized at each addition. In Figures 20, the amperometry and respective calibration curve for the bioelectrode PGE-rGO-MWCNTs-PBSE-BOX is presented.

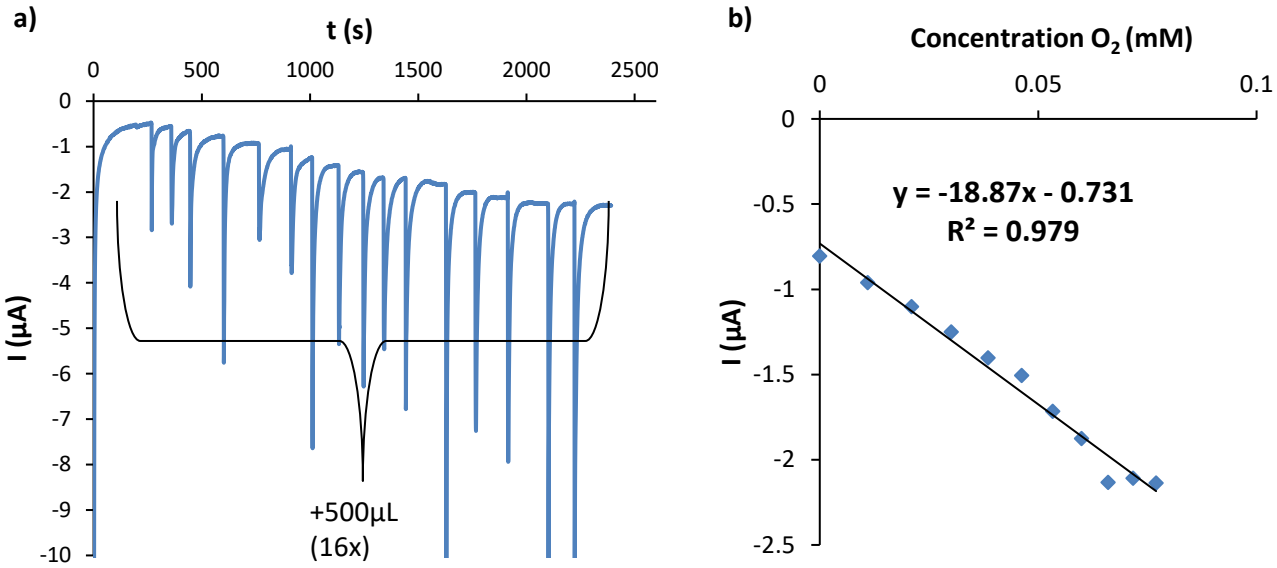

Figure 20- Amperometry (a) and Calibration Curve (b) of PGE modified with rGO-MWCNTs-PBSE-BOx in presence of different concentration of dissolved oxygen; Electrolyte: 10 mM PBS pH 7 V=20000µL; C_{PBSE}: 10mM; Potential: 0.10 V.

The amperometry was repeated 3 times and the mean values were used for the construction of the calibration curve. Analytic data was obtained and presented in Table 7.

Table 7- Analytical parameters for the O_2 biosensor obtained by amperometry

Biocathode	Sensitivity ($\mu A.mM^{-1}.cm^2$)	LOD (mM)	LOQ (mM)
rGO-MWCNTs (DMF)-PBSE-BOx	601	0.10	0.30

The sensitivity of the biosensor is a measure of its ability to discriminate between small differences in analyte concentration and it was calculated according to the equation 2 [118; 119]:

$$Eq\ 2: \qquad Sensitivity = \frac{m}{A_{Surface}}$$

where m refers to the calibration curve Slope (in µA.mM^{-1}), $A_{Surface}$ is the electrode surface area (0.0314 cm^2 corresponding to the PGE active surface area).

The Limit of Detection (LOD) is the lower concentration of analyte that can be detected with a certain level of trust or even distinguish from noise. The Limit of Quantification (LOQ) is the lower concentration of analyte that can be quantified with a certain level of trust. Both LOD and LOQ were calculated based on the equation 3 [120]:

$$Eq\ 3: \qquad LOD = \frac{K \times S_x}{m}$$

where LOD refers to the limits (in mM), S_x is the standard derivation of the response of the blank (without O_2), m is the calibration curve Slope and K is the coefficient. K value is equal to 3.3 for the determination of LOD and 10 for LOQ. The standard deviation of the blank was determined by measuring the signal of the blank between 253 and 269 seconds of the amperometric curve, which corresponded to a standard deviation value of 0.57 µA.

Considering the results obtained in Table 7, the sensitivity obtained (600 µA.mM^{-1}.cm^{-2}) is relatively high by the fact that some articles refer to sensitivities values of many biosensors in a range between 1 to 400 µA.mM^{-1}.cm^{-2} [121]. The achieved sensitivity of the tested biosensor (PGE-rGO-MWCNTs-PBSE-BOx) is higher when compared with other oxygen biosensors in the literature [122; 123].

The obtained results confirm the good efficiency of bioelectrodes PGE-rGO-MWCNTs-PBSE-BOx on the electrocatalysis of the enzyme-substrate O_2 and therefore was used as a biocathode for the construction of Glucose/O_2 biofuel cell.

3.2.2. Characterization of GOx Bioelectrodes Used as a Biosensor for Glucose Detection

For the fabrication of the glucose bioelectrode, GOx enzyme was used for the bioelectrocatalysis process in a similar immobilization process. In this case, SWCNTs were employed instead of MWCNTs since redox peaks of the catalytic center of the enzyme gave more well-defined (results not shown). CV analysis was done in order to assess an efficient immobilization of the enzyme to the electrode surface through PBSE cross-linking. Two different assets were performed such as the non-modified electrode (sensor) and the modified electrode with GOx immobilized on the surface (biosensor).

The biosensor was tested in the presence and absence of glucose while the sensor was only tested in the presence of glucose (Figure 21).

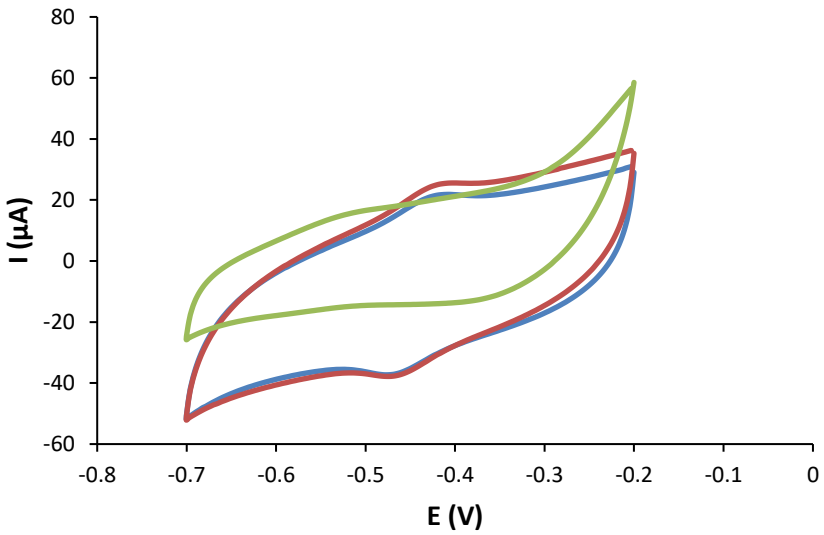

Figure 21- Cyclic Voltammograms of PGE-SWCNTs-PBSE-GOx in presence of glucose (–), PGE-SWCNTs-PBSE-GOx in absence of glucose (–) and PGE-SWCNTs-PBSE in presence of glucose (–); Electrolyte: 0.1 M PBS pH 7 with 10 mM glucose; Scan rate: 20 mV.s^{-1}.

The appearance of redox peaks for the bioelectrode PGE-SWCNTs-PBSE-GOx in the absence of substrate is attributed to the catalytic center of the enzyme GOx, which indicates efficient immobilization of the enzyme to the electrode surface in DET mode (without mediator). The results on the PGE-SWCNTs-PBSE sensor do not show the redox peaks and the current capacity is lower. Without the enzyme immobilized on the sensor surface, the catalyze reaction can't be achieved. As for the PGE-SWCNTs-PBSE-GOx biosensor, the redox peaks can be seen around -0.45 V. The oxidation current peak obtained for the biosensor tested in the presence of glucose is 16% greater compared to the same biosensor in the absence of glucose, indicating that the enzyme is catalyzing the glucose. As reported by some authors, sequential additions of the substrate lead to an increasing of catalytic currents and consequently an increase of current peaks [124; 125; 126].

This analysis was also performed in the presence of a mediator (benzoquinone) dissolved in the electrolyte (Figure 22).

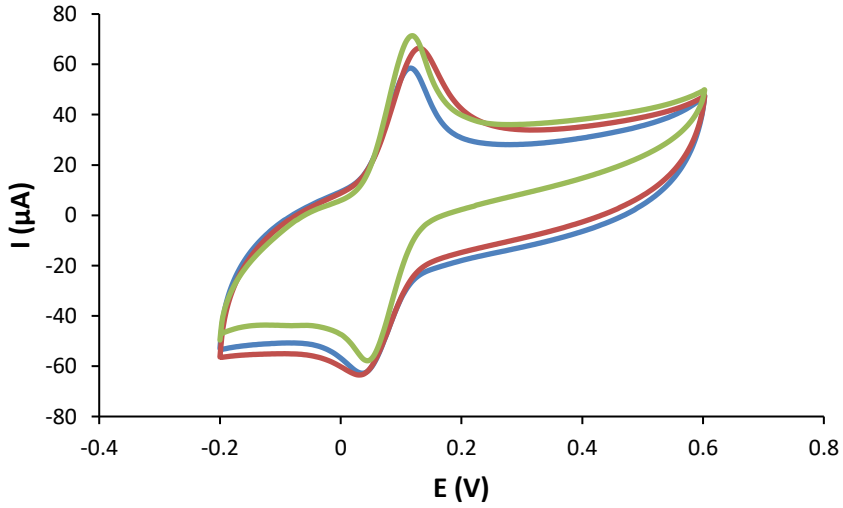

Figure 22- Cyclic Voltammograms of PGE-SWCNTs-PBSE-GOx in presence of glucose (–), PGE-SWCNTs-PBSE-GOx in absence of glucose (–) and PGE-SWCNTs-PBSE in presence of glucose (–); Electrolyte: 0.1 M PBS pH 7 with 2 mM benzoquinone and 10 mM glucose; Scan rate: 20 mV.s^{-1}.

The redox peaks observed in the CVs of Figure 22 represent a typical response of the benzoquinone mediator [127]. Considering the biosensor, in the presence of glucose there is a shift in the oxidation signal. The oxidation current peak of the sensor (without GOx) is ≈7% higher than the biosensor in the presence of glucose with also better-defined peaks. This phenomenon could be explained by some electrical resistance attributed to the enzymes due to their insulating glycoproteic shell [128].

The presence of the enzyme onto the electrode surface enhanced the oxidation catalytic current of glucose. Considering the attained biosensor results, the presence of glucose shifted the oxidation peak from +0.10 V to +0.13 V and increased the current peak in 17%, when compared in the absence of glucose. Those results may indicate that the enzyme is, indeed, catalyzing the glucose.

Amperometric detection of glucose was then performed with bioelectrodes PGE-SWCNTs-PBSE-GOx and PGE-rGO-SWCNTs-PBSE-GOx with the respective results being presented in Figure 23 and Figure 24. A potential of about -0.4 V was used for the measurements accordingly with the oxidation peak verified in Figure 21. In DET mode, the bioelectrodes presented some stability problems, especially the one with both rGO and SWCNTs as observable in the initial phase of the amperometry of Figure 24a. This may be due to the high negative potential value used or biofilm instability. Nevertheless, at a given concentration the current tends to less negative values indicating the oxidation of glucose. The sensitivity obtained from the slope of the calibration curve (Figure 23b and Figure 24b) was higher for the bioelectrode PGE-rGO-SWCNTs-PBSE-GOx, corresponding to 2.78 $\mu A.mM^{-1}$ compared to the one without rGO (0.82 $\mu A.mM^{-1}$). However, the LOD value was worse due to the higher value of the standard deviation of the blank response caused by the initial amperometric instability.

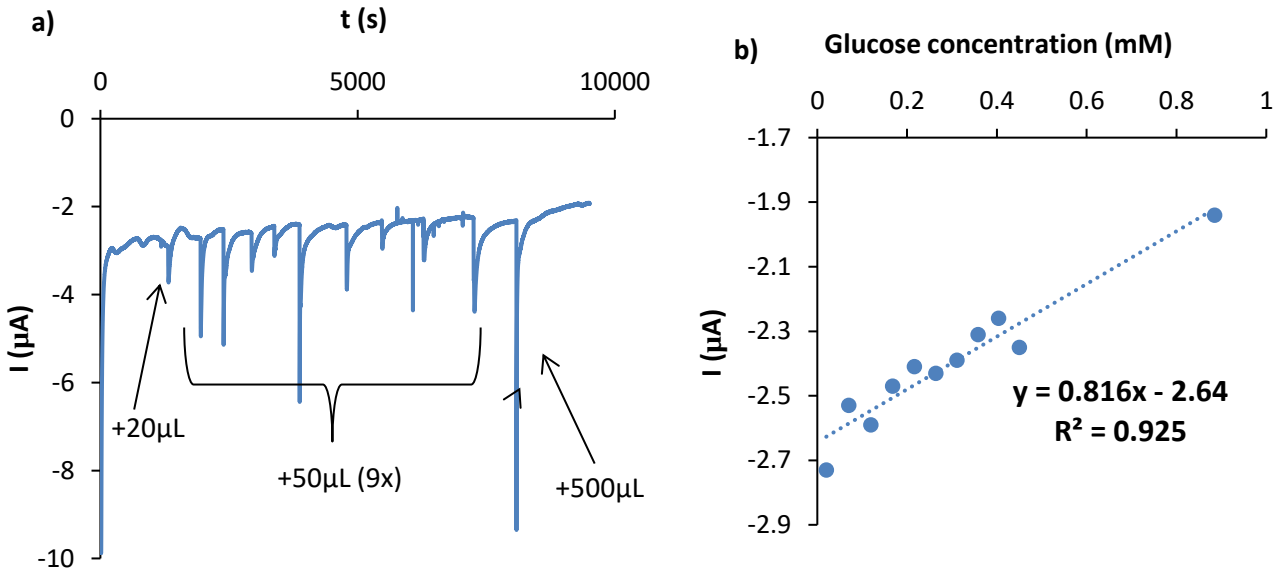

Figure 23- Amperometry (a) and Calibration Curve (b) of PGE-SWCNTs-PBSE-GOx in presence of different concentration of glucose; Electrolyte: 0.1 M PBS pH 7; Additions of 10 mM glucose solution; Potential: -0.41 V.

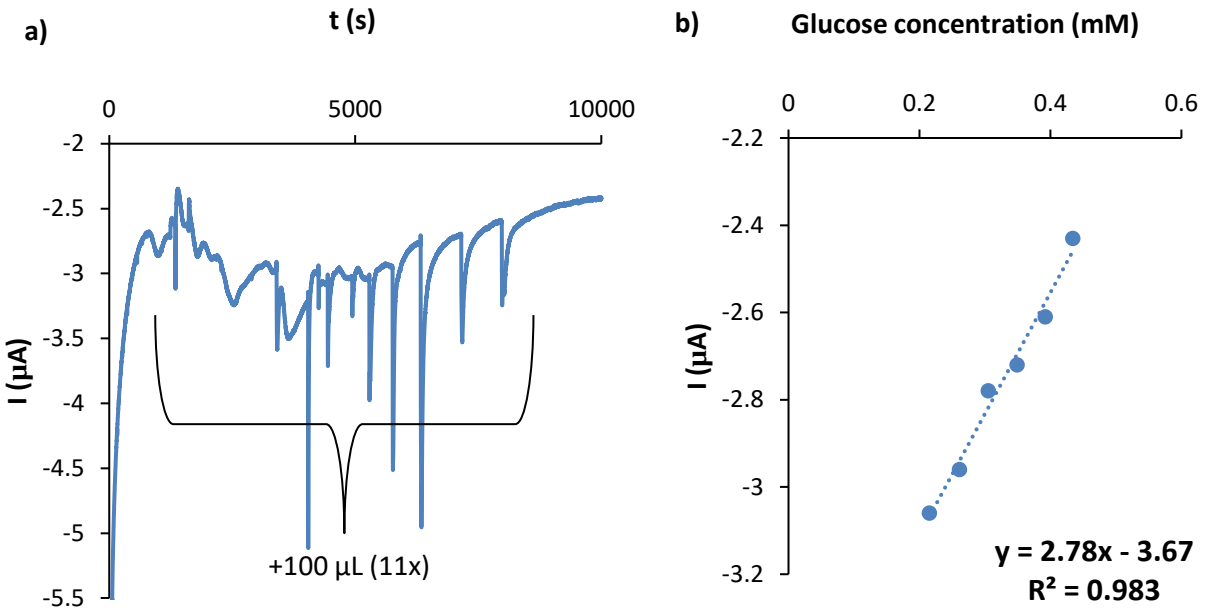

Figure 24- Amperometry (a) and Calibration Curve (b) of PGE-rGO-SWCNTs-PBSE-GOx in presence of different concentration of glucose; Electrolyte: 0.1 M PBS pH 7; Additions of 10 mM glucose solution; Potential: -0.35 V.

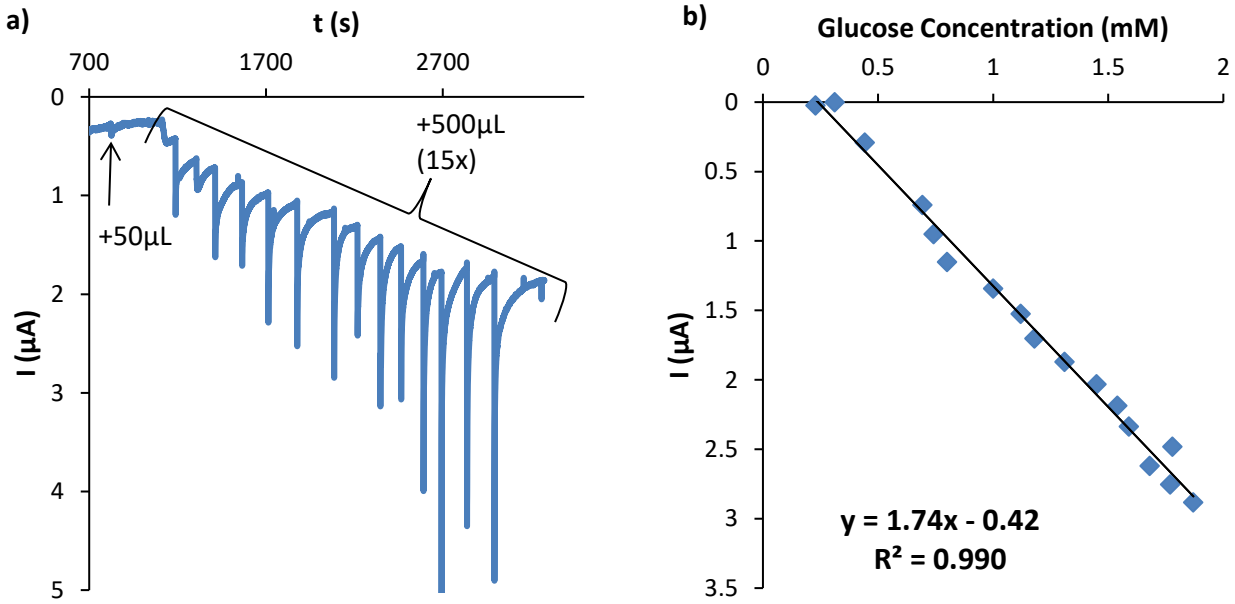

Figure 25- Amperometry (a) and Calibration Curve (b) of PGE-SWCNTs-PBSE-GOx in presence of mediator and different concentration of glucose; Electrolyte: 0.1 M PBS pH 7; with 2 mM benzoquinone; Additions of 10 mM glucose solution; Potential: +0.14 V.

The amperometric detection of glucose was also performed in the presence of the mediator (Figure 25) where the potential value selected corresponded to +0.14 V, as seen in Figure 22. The stability of the bioelectrode was higher in MET conditions as observable by the behavior of the amperometric curve (Figure 25a) and as well by the correlation of the calibration curve presented in Figure 25b (R^2 = 0.99).

The analytical parameters of all the amperometric measurements are presented in Table 8.

Table 8-Analytical parameters for the glucose biosensor obtained by amperometry

Bioanode	Sensitivity ($\mu A.mM^{-1}.cm^2$)	LOD (mM)	LOQ (mM)
PGE-SWCNTs-PBSE-GOx	26.0	0.04	0.12
PGE-rGO-SWCNTs-PBSE-GOx	88.5	0.15	0.44
PGE-SWCNTs-PBSE-GOx (with BQ)	55.4	0.09	0.28

Briefly analyzing Table 8, the double-layer biosensor obtained the highest sensitivity value. Also, it can be observed that the presence of a mediator increases the sensitivity of the biosensor by 113% when comparing biosensors without employing rGO. Also achieved the best R^2 and wider linear range as well as good values of sensitivity, LOD and LOQ. In terms of LOD, the biosensor PGE-SWCNTs-PBSE-GOx achieved the lowest value.

The determined sensitivity of the tested biosensors was relatively low in comparison with the glucose-based biosensors encountered in the literature, where values of sensitivity may vary in a range between 1 to 400 $\mu A.mM^{-1}.cm^{-2}$ [121]. For example, in Lee et al. [129] a titania nanotubes array film with GOx achieved sensitivity close to 45 $\mu A.mM^{-1}.cm^{-2}$. However, many studies have reported sensitivities lower than 40 $\mu A.mM^{-1}.cm^{-2}$ for modified electrodes based on MWCNTs and rGO [130].

Although the enzyme GOx was well immobilized in the electrode surface, showing evidence of DET, the detection of GOx substrate in these conditions were not the most reproducible. In this respect, the use of a mediator can facilitate the electron transfer and improve the detection conditions though at the expense of using an additional reagent.

3.3. Characterization of the Bioanode and Biocathode and Assembly of the Biofuel Cell

The third stage of this work consists in the assembly of a glucose/O_2 biofuel cell using the previously characterized bioelectrodes as biocathode and bioanode. First, biocathode and bioanode were individually characterized through the determination of the polarization curves.

A polarization curve is one of the most common methods of testing a (bio)fuel cell, allowing easy comparison to other published polarization curves and may also be useful for troubleshooting issues in the cell stack. The polarization curve displays the voltage output of

the (bio)fuel cell for a given current density loading. Also, it can be considered as the basic kinetic law for any electrochemical reaction [131].

Polarization curves are usually obtained with a potentiostat/galvanostat, which draws a fixed current from the (bio)fuel cell and measure the output voltage and by slowly "stepping up" the load on the potentiostat, the voltage response can be determined [132]. In this work, the polarization curves were obtained using linear sweep voltammetry (LSV) technique, where the current at a working electrode is measured while the potential between the working electrode and a reference electrode is swept linearly in time [133].

Figure 26 is a classic representation of a polarization curve, where it can be observed three distinct regions such as activation polarization, ohmic polarization, and concentration polarization, which represents the main potential drops at low current densities, moderate current densities, and high current densities respectively. Those voltage losses depend on operating conditions such as temperature, the load applied, and fuel/oxidant flow rates. Generally, activation losses are related to the voltage overpotential required to overcome the activation energy of the electrochemical reaction on the catalytic surface. The ohmic losses can be defined as electrical resistance in the cell components such as electrolyte, catalytic layer, terminal connections, etc. For last, the concentration losses exist due to mass transport of uncharged species like product and residue that shall be removed continuously to maximize the (bio)fuel cell efficiency [131].

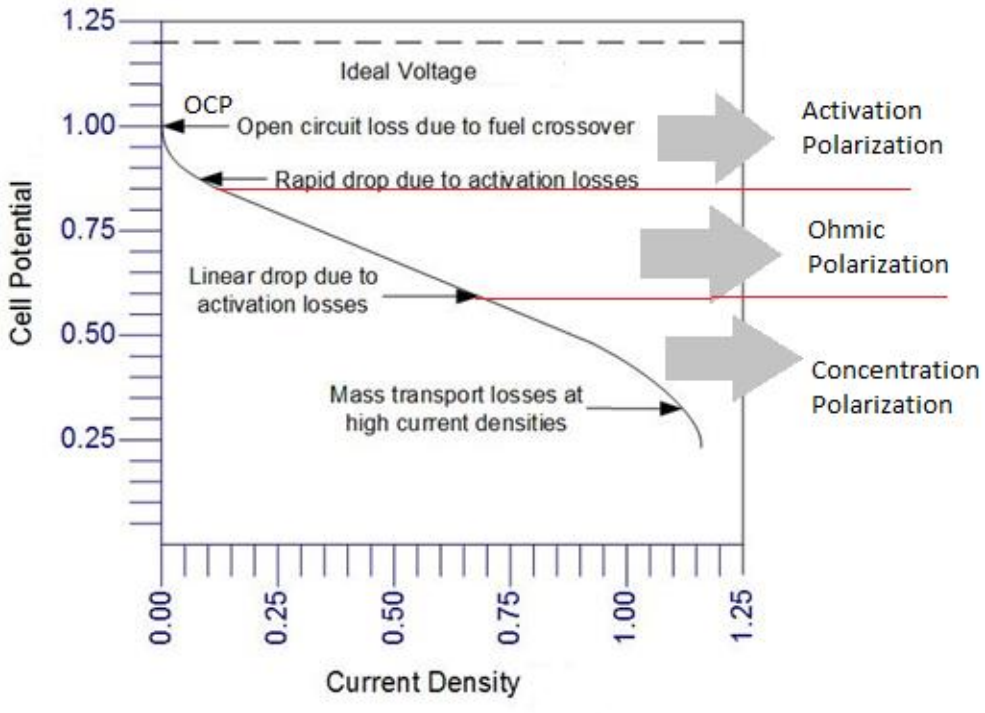

Figure 26- Representation of a typical polarization curve, based on [131; 134].

The fixed current potential applied corresponds to the open circuit potential (OCP), which is the potential established between the working electrode and the environment, concerning a reference electrode. In another way, it is the potential value in an open circuit (with no applied

voltage). OCP represents the maximum potential that a certain biosensor can handle in the cell [135].

Values of OCP can alter depending on the cell components particularly the electrodes and electrolyte. Their respective composition, the occurrence of certain reactions as well as the presence of (un)charged species may have an impact on the electron transfer system. For example, some studies confirmed that the corrosion phenomenon on the electrode surface tends to decrease the OCP value [135; 136]. Like the polarization curves, the OCP can give important information about the redox state of species in the bulk solution

In Figure 27, the polarization curve of the biocathode PGE-RGO-MWCNTs-PBSE-BOx in air-saturated buffer in DET mode is represented. The OCP of the biocathode corresponds to 0.53 V and the generated maximum current density corresponded to 172 µA.cm^{-2} at 0 V. The presence of substrate results in eligible catalytic activity, enhancing the electron transfer system. The curve without O_2 was not determined, however, in theory it was expected to provide similar OCP but much lower current density value.

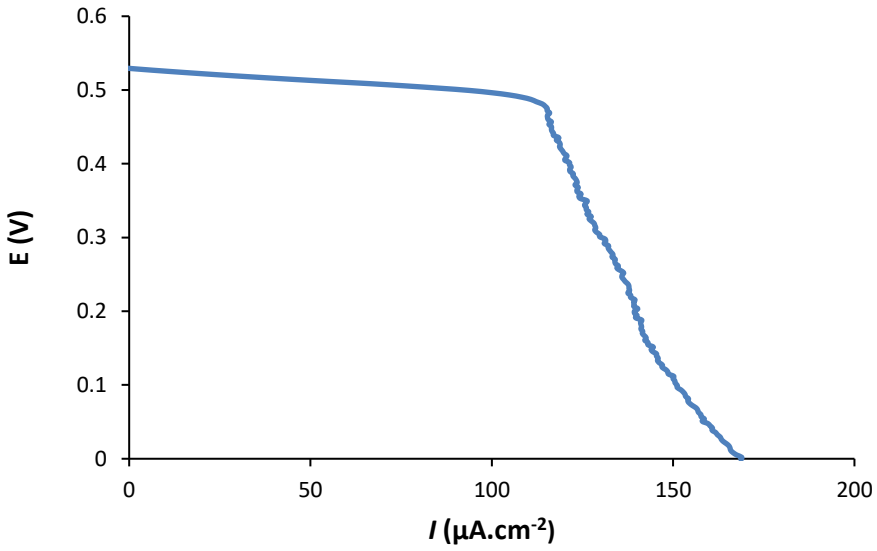

Figure 27- Polarization curve of the biocathode composed with PGE-rGO-MWCNTs-PBSE-BOx; Biocathode was tested in air saturated buffer. Electrolyte: 0.1 M PBS pH 7; Scan rate: 1mV.s^{-1}. .

The establishment of DET between PGE and BOx makes possible the application of the bioelectrode as a biocathode in membraneless biofuel cells. In the literature, it is possible to find examples of PGE-based or BOx based biocathodes. For example, a mediated PGE-MWCNTs with laccase immobilized achieved OCP of 0.58 V and maximum current density of 296 µA.cm^{-2}, while others BOx based biocathodes using PBSE achieved OCP of around 0.5 V and maximum current density of 200 µA.cm^{-2} [137; 138]. Interestingly, for analogues enzymes, the OCP is around 0.50 V however the maximum current density varies generally from 300 to

750 µA.cm^{-2}. In this work, the maximum value of the current density obtained for the biocathode was somewhat lower than the reported literature values [139; 140]. The main possible reason may be due to the oxygen concentration on the electrolyte. The electrolyte was air saturated and not O_2 saturated and so oxygen was present only at 21%.

Polarization curves of the bioanode PGE-rGO-SWCNTs-PBSE-GOx were obtained with DET and MET transfer systems and with absence and presence of glucose (Figure 28). Surprisingly, the reached results were contrary to what was expected since, in the presence of the substrate glucose, the OCP and current densities achieved were very low, even when using the mediator benzoquinone. To note also that the best current density values were achieved in the presence of the mediator and in the absence of the enzyme's substrate. These results may indicate that the immobilization method used for GOx is not the most effective for biofuel cell assemblies.

Although the immobilization method for GOx using PBSE was already been described in the literature [141; 142; 143], no works were found applied in biofuel cell studies. These experiments were performed in an electrolyte without O_2 since it is a co-substrate of GOx and may interfere in the electron transfer to glucose in biofuel cells. In this situation, O_2 probably should have been presented for the proper functioning of the enzyme catalysis.

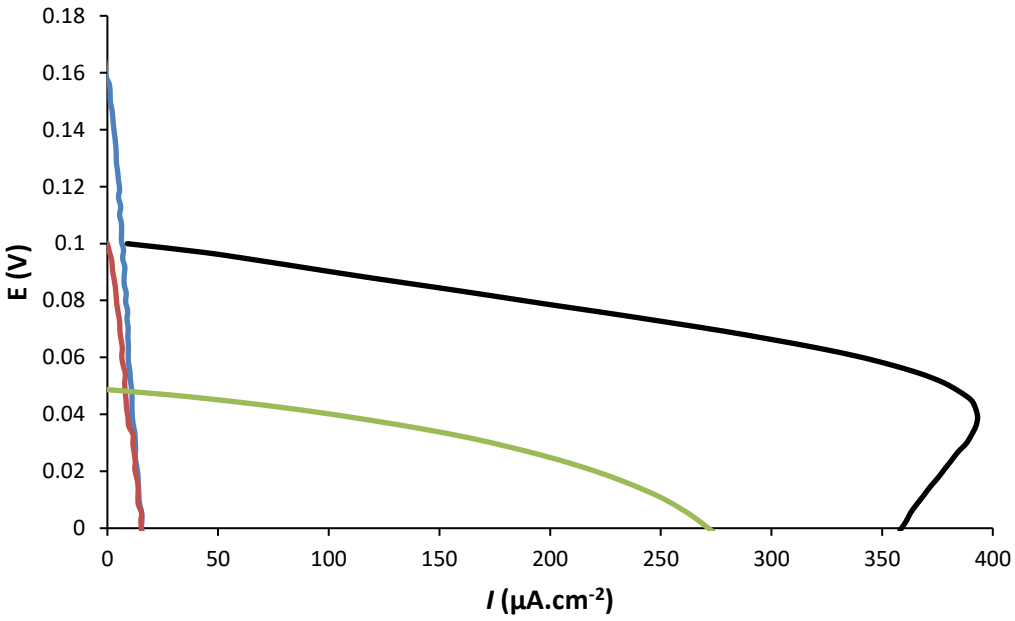

Figure 28- Polarization curve of the bioanode composed with PGE-rGO-SWCNTs-PBSE-GOx; Bioanode was tested in absence of glucose with mediator (–) and without mediator (–) and also in presence of glucose with mediator (–) and without mediator (–). Electrolyte: 0.1 M PBS pH 7 with 2 mM benzoquinone and 10 mM glucose in absence of dissolved O_2; Scan rate: 1mV.s^{-1}.

Regarding the results of the MET transfer system, the current density obtained was around 6 times bigger than DET, achieving a maximum of 250 µA.cm^{-2} for the anode in the presence of glucose. According to the literature, the purpose of the addition of a mediator is to increase

the electrotransfer system between the electrode surface and the electrolyte, enhancing the OCP and, consequently, improving the current density and power density [144]. The establishment of MET between PGE and GOx makes possible the application of the bioelectrode as a bioanode in membraneless biofuel cells.

In the literature, it is possible to find examples of GOx based bioanodes. For example, a CEC-CNTs-GOx in DET achieved an OCP of 0.43 V, current density around 600 $\mu A.cm^{-2}$ and power density 180 $\mu W.cm^{-2}$ [80] while a CNTs-GOx in MET achieved only an OCP of 0.24 V and a low power density around 0.28 $\mu W.cm^{-2}$ [145]. The different results between MET and DET electron transfer are indeed significant, like as stated on Fiorito et. Al [146], where a polypyrrole-GOx based electrode working in MET can achieve up to 300% higher current density than working in DET (max of 25 $\mu A.cm^{-2}$ at OCP 0.50 V). The disparities of results from these literature studies lead to suppose that immobilization strategy of GOx and working conditions are critical for the bioelectrode efficiency.

The final stage of this work consisted in the assembly of the glucose/O_2 biofuel cell, composed by a PGE-rGO-MWCNTs-PBSE-BOx and a PGE-rGO-SWCNTs-PBSE-GOx, as the biocathode and bioanode respectively. Accordingly, the biofuel cell was evaluated membraneless in PTN conditions. OCP value for the biofuel was determined first and then the polarization curve was obtained by LSV.

Figure 29a shows the polarization curve of the biofuel cell working in DET, while Figure 29b shows the respective power curves obtained from the determined polarization curves and accordingly to the following equation:

$$Eq\ 4: \quad P = I \times V$$

By multiplying the current density (I) with the voltage (V), the power density (P) can be estimated. Those graphics were obtained for various concentrations of glucose (0, 5, 10, and 50 mM) in air-saturated phosphate buffer solution pH 7.0 in the presence and absence of oxidant, O_2, dissolved in the electrolyte.

It can be noticed that the results for 5 mM of glucose in the presence of oxygen achieved the highest power density and OCP (5.77 $\mu W.cm^{-2}$ and 0.23 V respectively). Also, the maximum value for the current density is about 65 $\mu A.cm^{-2}$ and shows no significant variation with the glucose concentration. This suggests that saturation of GOx enzyme with glucose occurs in concentration around 5 mM or less as power density decreased with glucose concentration. There is a significant decrease in the achieved maximum power density and current density of around 300 to 400% when the fuel solution has no O_2. This was expected since no (or negligible) oxidant was present in the solution in order to complete the circuit of electrons flow.

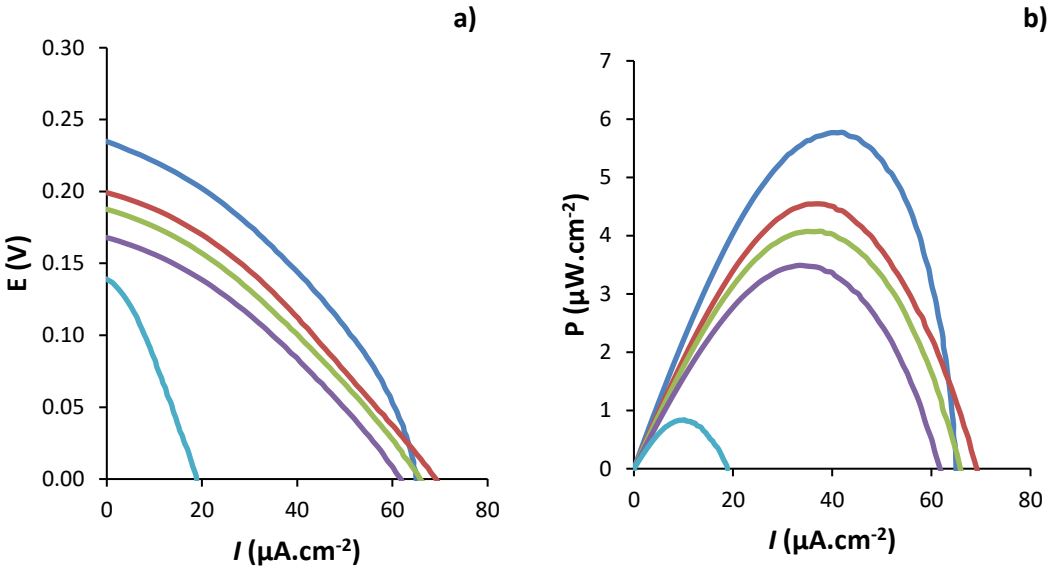

Figure 29- Performance of the Biofuel Cell working on DET: a) Polarization curves; b) Power density curves. Conditions: air-saturated with dissolved O_2 and different concentrations of glucose [0 mM (—), 5 mM (—), 10 mM (—) and 50 mM (—)] and in absence of O_2 with 50 mM glucose (—). Electrolyte: 0.1 M PBS pH 7; Scan rate: 1 $mV.s^{-1}$.

Figure 30a shows the polarization curve of the biofuel cell working in MET, while Figure 30b shows the respective power curve. Those graphics were obtained for various concentrations of glucose (5, 10, and 50 mM) in air-saturated phosphate buffer solution pH 7.0 containing or not dissolved O_2.

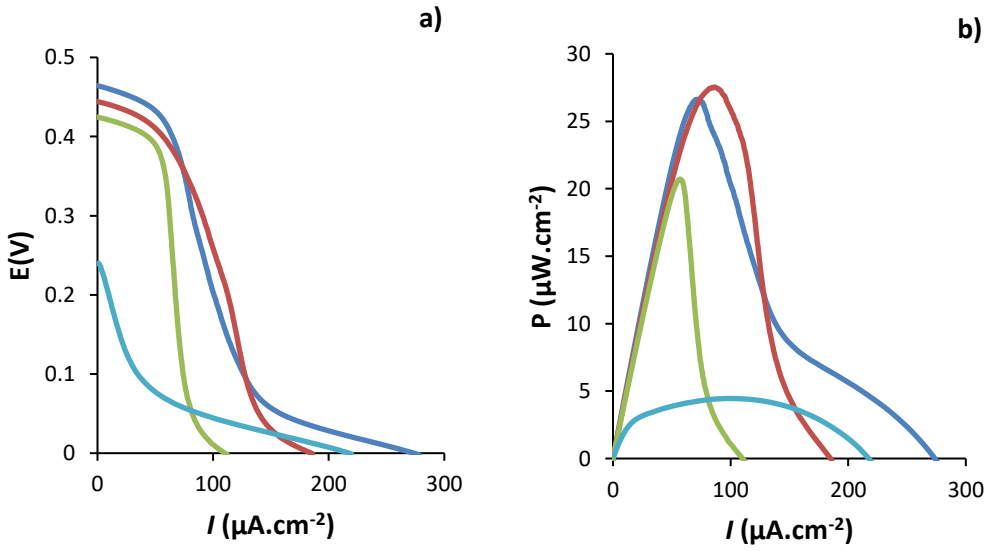

Figure 30- Performance of the Biofuel Cell working on MET: a) Polarization curves; b) Power density curves. Conditions: air-saturated with dissolved O_2 and different concentrations of glucose [5 mM (—), 10 mM (—) and 50 mM (—)] and in absence of O_2 with 50 mM glucose (—). Electrolyte: 0.1 M PBS pH 7; Mediator: 2 mM Bezoquinone; Scan rate: 1 $mV.s^{-1}$.

It can be noticed that the results for 10 and 50 mM of glucose in presence of oxygen achieved the highest power density and OCP (around 26 $\mu W.cm^{-2}$ and 0.42 V respectively). The power density for 50 mM glucose was similar to 10 mM glucose, which suggests that a saturation point was achieved with 50 mM concentration. Also, the maximum value for current density is about 264 $\mu A.cm^{-2}$ and it varies with the glucose and oxygen concentration. The absence of oxygen also decreased the power and current density, in a similar way that it was observed in DET (Figure 29).

As observable in these results the presence of a mediator facilitates the electron transfer, increasing the output values. So, the results on MET achieved better power and current density about 4 to 7 times better than the DET results. The biofuel cell underperformed in DET mode clearly due to the limitations in the anode side as was discussed earlier in the individual characterization of the bioanode.

It is important to note that the DET feature is always preferable to MET since no additional compounds are used. This is especially relevant if diffusional mediators are used since cross-over to the other electrode may create undesirable electron pathways and lead to decreases in power output. Moreover, oxygen is also a co-substrate of GOx enzyme which can lead to interference in the catalysis of glucose, resulting in a reduction of the power output of the biofuel cell [147]. Therefore, some works stated that high concentrations of oxygen can also lead to undesirable electron transfer, resulting in the reduction of power output as well [148].

The best result obtained is compatible with some similar glucose/O_2 biofuel cells based on GOx and BOx [64; 67; 149]. However, certain works present better OCP and power density values when alternatives enzymes are used, especially for the bioanode construction [70; 74; 79].

4. Conclusion and Future Perspectives

It is evident the necessity to lower dependence on fossil fuels on our energy demand in order to attain environmental sustainability and consequently economical and societal sustainability. So, an increasing investment must be done on the already established renewable-energy technologies as well as on new and potential alternative sources. The work developed here is an attempt to contribute to biofuel cell technology as an alternative and sustainable energy conversion systems.

Here, a membraneless glucose/O_2 biofuel cell was successfully developed employing enzymes as biocatalysts for the conversion of chemical energy into electrical one and also pencil graphite as an inexpensive and ubiquitous transducer material.

The selection of pencil graphite electrodes as a transducer for enzyme immobilization was well justified through voltammetric characterization with the obtained electrochemical parameters being compared with more conventional type electrodes. With the purpose to enhance the electrochemical properties of PGE sand to effectively immobilize enzymes to the electrode, some widely used carbon materials were assessed. It was clearly evident the synergetic effect of reduced graphene and carbon nanotubes on the obtained signal and therefore implemented in the nanostructuration of PGE.

A simple chemical immobilization method was adopted for the attachment of both enzymes glucose oxidase and bilirubin oxidase to the modified PGE surface by using a cross-linker compound. This method revealed to be extremely efficient in the immobilization of BOx since the DET feature was assessed easily and presented an excellent analytical performance in the detection of its substrate, O_2. However, regarding the immobilization of GOx some instability and unreproducible results were observed in the analytical performance towards glucose. One aspect to take into account is the influence of O_2 in the catalysis of glucose by GOx and this was not assessed as all experiments considering the analysis of glucose were performed in the absence of O_2.

This limitation on the bioanode side was also evident in the assembly of the membraneless biofuel cell working in DET mode, as the maximum power produced was only about 6 $\mu W.cm^{-2}$. This was in part minimized by the introduction of a diffusional mediator to facilitate the electron transfer on the anode side which raised the maximum power density produced to about 26 $\mu W.cm^{-2}$. However, the membraneless configuration of the biofuel cell may allow cross-reactions of the mediator at the cathode which lowers the power output. Also, another concern is the sensitivity of GOx to O_2 as this molecule is also a co-substrate of the enzyme. As O_2 is indispensable at the biocathode and again the absence of membrane may contribute to the undesirable transference of electrons between O_2 and the bioanode lowering the expected power output.

Other enzymes may be suitable and appropriate in this type of configuration. For instance, glucose dehydrogenase enzyme also catalyzes glucose, however, is insensitive to O_2. Also, this enzyme has a higher capability to perform DET catalysis in a more efficient way.

Biofuel cells with membraneless configuration are always desirable as they are more simply fabricated and can be miniaturized. In order to attain maximum efficiency in this type of biofuel cell, the use of diffusional mediators should be avoided. For miniaturization purposes, PGE seems to be an adequate transducer as they are available in various sizes and are easily modifiable.

Nowadays, the field of the biofuel cell is growing due to improvements in the immobilization efficiency. However, the level of stability that limits biofuel cell utilization and market implementation is still a challenge to be properly addressed, especially regarding the viability power generation using residues and waste products as fuel or application as implantable devices.

5. Bibliography

1. **Fanchi, J.R.,** *Energy in the 21st Century.* Vol. 4. 2010: Worlds Scientific. DOI: 10.1142/10160;

2. *RENEWABLES 2019: GLOBAL STATUS REPORT.* 2019, REN21.

3. *Energy statistics - an overview.* Eurostat. [Online] August 1, 2019. [Cited: December 9, 2019.] Link: https://ec.europa.eu/eurostat/statistics-explained/index.php?title=Energy_statistics_-_an_overview#Energy_dependency.

4. **Yang, Xiao-Yu, et al**., *Immobilization technology: a sustainable solution for biofuel cell design.* Energy & Environmental Science. Royal Society of Chemistry, 2012. Vol. 5, Issue 2, p. 5540-5563. DOI: 10.1039/C1EE02391H.

5. **Abirami, et al.,** *Promising Trends In Green Power Technologies*. 1st International Conference on New Scientific Creations in Engineering and Technology, 2019 (March - 2019). ISSN: 2455-1457.

6. **Slate, A.J., et al.,** *Microbial fuel cells: An overview of current technology*. Renewable and Sustainable Energy Reviews. Elsevier, 2019. Vol. 101, p. 60-81. DOI: 10.1016/j.rser.2018.09.044.

7. *Global Warming of 1.5 ºC. 2018*, Intergovernmental Panel on Climate Change, IPCC.

8. **Winter, M. and R.J. Brodd,** *What Are Batteries, Fuel Cells, and Supercapacitors?* Chemical Reviews, ACS Publishing 2004. 104(10): p. 4245–4270. DOI: 10.1021/cr020730k.

9. **Yadav, M., et al.,** *Biofuel Cells: Concepts and Perspectives for Implantable Devices, i*n Biofuels: Production and Future Perspectives, R.S. Singh; A. Pandey; and E. Gnansounou;, Editors. 2017, CRC Press. Vol.1, Chapter 21, p. 541-566.

10. **Bullen, R.A., et al.,** *Biofuel cells and their development.* Biosensors and Bioelectronics, 2006. Vol. 21(11): p. 2015-2045. DOI: 10.1016/j.bios.2006.01.030.

11. **Zhu, Z., et al.,** *A high-energy-density sugar biobattery based on asynthetic enzymatic pathway.* NatureResearch Journal, 2013. Vol. 5(3026). DOI: 10.1038/ncomms4026.

12. **Kerzenmacher, S., et al.,** *Biofuel cells for the energy supply of distributed systems: State-of-the-Art and applications.* Sensoren und Messsysteme, 2010. Vol. 18: p. 562-565.

13. **Thévenot, D.R., et al.,** *Electrochemical biosensors: recommended definitions and classification.* Pure and Applied Chemistry 71, 1999. Vol. 16(1-2): p. 121-131. DOI: 10.1016/S0956-5663(01)00115-4

14. **Minteer, S.D., B.Y. Liaw, and M.J. Cooney,** *Enzyme-based biofuel cells,* in Current Opinion in Biotechnology, G. Stephanopoulos; and J.R.v.d. Meer;, Editors. 2007, Elsevier. p. 228-34. DOI: 10.1016/j.copbio.2007.03.007.

15. **Falk, M., et al.,** *Biofuel Cells for Biomedical Applications: Colonizing the Animal Kingdom.* Chemphyschem, 2013. Vol. 14(10): p. 2045-2058. DOI: 10.1002/cphc.201300044.

16. **Davis, F. and S.P.J. Higson**, *Advances and applications in biofuel cells,* in Handbook of Bioelectronic, S. Carrara; and K. Iniewski;, Editors. 2015, Cambridge University Press. p. 201-214. DOI: 10.1017/CBO9781139629539.019.

17. **Slaughter, G. and T. Kulkarni,** *Enzymatic Glucose Biofuel Cell and its Application.* Journal of Bioengineering and Bioelectronics, 2015. Vol. 5(1): p. 1000110. DOI: 10.4172/21530777.1000111.

18. **Kerzenmacher, S.,** *Biofuel cells as sustainable power sources for implantable systems,* in Implantable Sensor Systems for Medical Applications, A.I. ; and D. Hodgins;, Editors. 2013, Woodhead. p. 183-212. DOI: 10.1533/9780857096289.1.183.

19. **MacVittie, K., et al.,** *From "cyborg" lobsters to a pacemaker powered by implantable biofuel cells.* Energy & Environmental Science 2013. Vol. 6(1): p. 81-86. DOI: 10.1039/C2EE23209J.

20. **Rapoport, B.I., J.T. Kedzierski, and R. Sarpeshkar**, *A Glucose Fuel Cell for Implantable Brain–Machine Interfaces.* PLOS ONE, 2012. Vol. 7(6): p. e38436. DOI: 10.1371/journal.pone.0038436.

21. **Cosnier, S., A.L. Goff, and M. Holzinger,** *Towards glucose biofuel cells implanted* in human body for powering artificial organs: Review. Electrochemistry Communications;, 2014. Vol. 38: p. 19-23. DOI: 10.1016/j.elecom.2013.09.021.

22. **Gotovtsev, P., et al.,** B*ioenergy Based Power Sources for Mobile Autonomous Robots: Review.* Robotics, 2018. Vol. 7(2): p. 1-18. DOI: 10.3390/robotics7010002.

23. **Parent, A., Giovanni Aldini:** *From animal electricity to human brain stimulation.* The Canadian Journal of Neurogical Sciences, 2004. Vol. 31(4): p. 576-584. DOI: 10.1017/S0317167100003851.

24. **Piccolino, M.,** *Luigi Galvani and animal electricity: Two centuries after the foundation of electrophysiology.* Trends Neurosci, 1997. Vol. 20(10): p. 443-448. DOI: 10.1016/S0166-2236(97)01101-6.

25. **Potter, M.C.,** *Electrical effects accompanying the decomposition of organic compounds.* The Royal Society: Proceedings of the royal society B- Biological Sciences, 1911. Vol. 84: p. 260-279. DOI: 10.1098/rspb.1911.0073.

26. **Cohen, B.,** *The bacterial cell as an electrical half cell.* Journal of Bacteriology, 1935. Vol. 21: p. 18-19.

27. **Dell Duca, M.G. and J.M. Fuscoe,** *Thermodynamics and applications of bioelectrochemical energy conversion systems.* 1967, Washinton D.C.: National Aeronautics and Space Administration (NASA).

28. **Davis, J.B. and J.M. Yarbrough,** *Preliminary Experiments on a Microbial Fuel Cell.* Science, 1962. Vol. 137(3530), Issue.24, p. 615-616. DOI: 10.1126/science.137.3530.615.

29. **Clark, L.C. and C. Lyons,** *Electrode Systems for Continuous Monitoring* in Cardiovascular Surgery. AnnNY AcadSci, 1962. Vol. 31(102): p. 29-45. DOI: 10.1111/j.1749-6632.1962.tb13623.x.

30. **Updike, S.J. and G.P. Hicks**, *The enzyme Electrode.* NatureSearch Journal, 1967. Vol. 214: p. 986–988(1967).

31. **Shleev, S.A., et al.,** *Direct electron transfer reactions of laccases from different origins on carbon electrodes.* Bioelectrochemistry, 2005. Vol. 67(1): p. 115-124. DOI: 10.1016/j.bioelechem.2005.02.004.

32. **Shleev, S., et al.,** *Direct electron transfer between copper-containing proteins and electrodes.* Biosensors and Bioelectronics, 2005. Vol. 20(12): p. 2517-2554. DOI: 10.1016/j.bios.2004.10.003.

33. **Katz, E., I. Willner, and A.B. Kotlyar,** *A non-compartmentalized glucose vertical bar O2 Biofuel cell by bioengineered electrode surfaces.* J. Electroanal Chem., 1999. Vol. 479: p. 64-68.

34. **Katz, E., A.F. Buckmann, and I. Willner**, *Self-powered enzyme-based biosensors.* J. Am. Chem. Soc., 2001. Vol. 123(43): p. 10752–10753. DOI: 10.1021/ja0167102.

35. **Mano, N., F. Mao, and A. Helle,** *Characteristics of a miniature compartmentless glucose O2 biofuel cell and its operation in a living plant.* J. Am. Chem. Soc., 2003. Vol. 125(21): p. 6588–6594. DOI: 10.1021/ja0346328.

36. **Cinquin, P., et al.,** *A glucose biofuel cell implanted in rats.* PLoS one, 2010. Vol. 5(5): p. e10476. DOI: 10.1371/journal.pone.0010476.

37. **Inamuddin, et al.,** *Enzymatic Fuel Cells: Materials and Applications*. 2019: Materials Research Foundations. DOI: 10.21741/9781644900079. ISBN: 978-1-64490-006-2.

38. **Hitaishi, V.P., et al.,** *Controlling Redox Enzyme Orientation at Planar Electrodes.* Catalysts, 2018. Vo. 8(5): p. 192. DOI: 10.3390/catal8050192.

39. **Blanco, A. and G. Blanco,** *Medical Biochemistry.* Vol. 1. 2017: Academic Press. ISBN: 9780128035504.

40. **Gorton L, L.A., Larsson T, Munteanu FD, Ruzgas T, Gazaryan I.,** *Direct electron transfer between heme-containing enzymes and electrodes as basis for third generation biosensors.* Analytica Chimica Acta, 1999. Vol. 400(1-3): p. 91-108. DOI: 10.1016/S0003-2670(99)00610-8.

41. **Frey, P.A. and A.D. Hegeman,** *Enzymatic Reaction Mechanism.* Angewandte Chemie International Edition, 2007. Vol. 46(22): p. 7922-7924. DOI: 10.1002/anie.200785514.

42. **Cracknel, J.A., l.A. Vincent, and F.A. Armstrong**, *Enzymes as Working or Inspirational Electrocatalysts for Fuel Cells and Electrolysis.* Chemical Reviews, 2008. Vol. 108(7): p. 2439–2461. DOI: 10.1021/cr0680639.

43. **Ensafi, A.A.,** *Electrochemical Biosensors.* Vol. 1. 2019: Elsevier. ISBN: 9780128164914.

44. **Gorton, L.,** *Carbon paste electrodes modified with enzymes, tissues, and cells*. Electroanalysis, 1995. Vol. 7(2). DOI: 10.1016/S0003-2670(99)00610-8.

45. **Kłos-Witkowska, A.,** *Enzyme-Based Fluorescent Biosensors and Their Environmental,* Clinical and Industrial Applications. Pol. J. Environ. Stud, 2015. Vol.24: p. 19.25. DOI: 10.15244/pjoes/28352.

46. **Basso, A. and S. Serban,** *Industrial applications of immobilized enzymes—A review*. Molecular Catalysis, 2019. 479(110607): p. 2468-8231. DOI: 10.1016/j.mcat.2019.110607.

47. **Zhang, Y.-H.P., Myung, S., You, C., Zhu, Z., Rollin, J.A.,** *Toward low-cost biomanufacturing through in vitro synthetic biology: bottom-up design.* Journal of Materials Chemistry, 2011. Vol. 21(47): p. 18877-18886. DOI: 10.1039/C1JM12078F.

48. **Dominguez-Benetton, X., Srikanth, S., Satyawali, Y., Vanbroekhoven, K., Pant, D.,,** *Enzymatic electrosynthesis: an overview on the progress in enzyme electrodes for the production of electricity, fuels and chemicals.* Journal of Microbial & Biochemical Technology 2013. Vol. S6(007): p. 1-20. DOI: 10.4172/1948-5948.S6-007.

49. **Barsana, M.M., David, M., Florescu, M., Tugule, L., Brett, C.M.A.,,** *A new self-assembled layer-by-layer glucose biosensor based on chitosan biopolymer entrapped enzyme with nitrogen doped graphene.* Bioelectrochemistry, 2014. Vol. 99: p. 46-52. DOI: 10.1016/j.bioelechem.2014.06.004.

50. **Schuhmann, W., Lammert, R., Uhe, B., Schmidt, H.-L,** *Polypyrrole, a new possibility for covalent binding of oxidoreductases to electrode surfaces as a base for stable biosensors.* Sensors and Actuators B: Chemical, 1999. Vol. 1(1-6): p. 537-541. DOI: 10.1016/0925-4005(90)80268-5.

51. **Lotzbeyer, T., Schuhmann,W., Katz, E., Falter, J., Schmidt, H.L**. *Direct electron transfer between the covalenty immobilized enzyme microperoxidases MP-11 and a cytamine-modified gold electrode.* Jornal of Electroanalytical Chemistry, Elsevier, 1994. Vol. 377 (1-2) p. 291-294.DOI: /10.1016/0022-0728(94)03646-2.

52. **Yang, S.-T.**, *Bioprocessing for Value-Added Products from Renewable Resources.* Vol. 1. 2007: Elsevier. DOI: 10.1016/B978-0-444-52114-9.X5000-2.

53. **Zhang, Y., Liu, H., Yang, Z., Ji, S., Wang, J., Pang, P., Feng, L., Wang, H.,Wu, Z., Yang, W.,** *An acetylcholinesterase inhibition biosensor based on a reduced graphene oxide/silver nanocluster/chitosan nanocomposite for detection of organophosphorus pesticides.* Analytical Methods, 2015. Vol. 7(15): p. 6213-6219. DOI: 10.1039/C5AY01439E.

54. **Palod, P.A., Singh, V.,,** *Improvement in glucose biosensing response of electrochemically grown polypyrrole nanotubes by incorporating crosslinked glucose oxidase.* Materials Science and Engineering, 2015. Vol. 55: p. 420-430. DOI: 10.1016/j.msec.2015.05.038.

55. **Jørgensen, N.O.G.,** *Encyclopedia of Inland Waters: Carbohydrates*. 2009: Academic Press. p.727-742.

56. **Fry, E.L., J.R.D. Long, and R.D. Bardgett,** *Plant Communities as Modulators of Soil Carbon Storage,* in Soil Carbon Storage: , T.A. Ontl, Editor. 2018, Academic Press. p. 29-71. DOI: 10.1016/B978-0-12-812766-7.00002-0.

57. **Kuddus, M.,** *Enzymes in Food Biotechnology*. 2018: Academic Press.

58. **Wohlfahrt, G., et al.,** *1.8 and 1.9 A resolution structures of the Penicillium amagasakiense and Aspergillus niger glucose oxidases as a basis for modelling substrate complexes.* Biological Crystallography: Acta Crystallographica Section D, 1999. Vol. 55(5): p. 969-977. DOI: 10.1107/s0907444999003431.

59. **Wang, J.,** *Glucose Biosensors: 40 years of advances and challenges.* Electroanalysis, 2001. Vol.13(12). DOI: 10.1002/1521-4109(200108)13:12.

60. **Kulkarni, T. and G. Slaughte,** *Enzymatic Glucose Biofuel Cell and its Application*. Journal of biochips & tissue chips, 2015. Vol. 5(110). DOI: 10.4172/2153-0777.1000110.

61. **Cai, C., Chen, J.,** *Direct electron transfer of glucose oxidase promoted by carbon nanotubes.* Analytical Biochemistry, 2004. Vol. 332(1): p. 75-83. DOI: 10.1016/j.ab.2004.05.057.

62. **Sato, F., et al.,** *Enzyme-based glucose fuel cell using Vitamin K3-immobilized polymer as an electron mediator.* Electrochemistry Communications, 2005. Vol. 7(7): p. 643-647. DOI: 10.1016/j.elecom.2005.04.015.

63. **Chen, T., et al.,** *A Miniature Biofuel Cell*. Journal of the American Chemical Society, 2001. Vol. 123(35): p. 8630-8631. DOI: 10.1021/ja0163164.

64. **Lim, J., et al.,** *Nanostructured Sol-Gel Electrodes for Biofuel Cells*. Journal of The Electrochemical Society, 2006. Vol. 154(2): p. A140-A145. DOI: 10.1149/1.2404904.

65. **Saleh, F.S., L. Maoc, and T. Ohsaka,** *A promising dehydrogenase-based bioanode for a glucose biosensor and glucose/O2 biofuel cell.* Analyst,, 2012. Vol. 137(9): p. 2233. DOI: 10.1039/C2AN15971F.

66. **López-González, B., et al**., *Hybrid microfluidic fue lcell based on Laccase/C and AuAg/C electrodes.* Biosensors and Bioelectronics, 2014. Vol. 12(62): p. 221-226. DOI: 10.1016/j.bios.2014.06.054.

67. **Tsujimura, S., K. Kano, and T. Ikeda,** *Glucose/O2 Biofuel cell operating at physiological conditions.* Electrochemistry -Tokyo, 2002. Vol. 70(12): p. 940-942. DOI: 10.5796/electrochemistry.70.940.

68. **Campbell, A., et al.,** *Membrane/Mediator-Free Rechargeable Enzymatic Biofuel Cell Utilizing Graphene/Single-Wall Carbon Nanotube Co-Gel Electrodes.* Applied Materials & Interfaces, 2015. Vol. 7(7): p. 4056–4065. DOI: 10.1021/am507801x.

69. **Zhang, Y., et al.,** *Three-Dimensional Graphene Networks as a New Substrate for Immobilization of Laccase and Dopamine and Its Application in Glucose/O2 Biofuel Cell.* Applied Materials & Interfaces, 2014. Vol. 6(15). DOI: 10.1021/am502791h.

70. **Kang, Z., Y.-H.P.J. Zhang, and Z. Zhu,** *A shriveled rectangular carbon tube with the concave surface for high-performance enzymatic glucose/O2 biofuel cells.* Biosensors and Bioelectronics, 2019. Vol. 132: p. 76-83. DOI: 10.1016/j.bios.2019.02.044.

71. **Crepaldi, C.B., et al.,** *Ferrocene Entrapped In Polypyrrole Film and PAMAM Dendrimers as Matrix for Mediated Glucose/O2 Biofuel CellL,* in Electrochimica Acta, Vol.136 52–58. 2014, Elsevier.

72. **Liua, J., et al.,** *High-performance bioanode based on the composite of CNTs-immobilized mediator and silk film-immobilized glucose oxidase for glucose/O2 biofuel cells.* Biosensors and Bioelectronics, 2012. Vol. 15(31): p. 170–175. DOI: 10.1016/j.bios.2011.10.011.

73. **Ji, Y., et al.,** *A Fe3O4–carbon nanofiber/gold nanoparticle hybrid for enzymatic biofuel cells with larger power output.* Journal of Materials Chemistry A, 2017. Vol. 5(22): p. 11026-11031. DOI: 10.1039/C7TA01931A.

74. **Hui, Y., et al.,** *Three-Dimensional Nickel Foam Based Enzymatic Electrode and Its Glucose/O2 Biofuel Cell with High Power Density.* Journal of The Electrochemical Society, 2017. Vol. 13(164): p. G112-G120. DOI: 10.1149/2.0761713jes.

75. **Kanga, Z., et al.,** *Graphene oxide-supported carbon nanofiber-like network derived from polyaniline: a novel composite for enhanced glucose oxidase bioelectrode performance.* Biosensors and Bioelectronic, 2017. Vol. 96: p. 367-372. DOI: 10.1016/j.bios.2017.05.025.

76. **Zebda, A., et al.**, Single Glucose Biofuel Cells Implanted in Rats Power Electronic Devices. Scientific Reports, 2013(3): p. 1516. DOI: 10.1038/srep01516.

77. **Schubart, I.W., G. Göbel, and F. Lisdat,** *A pyrroloquinolinequinone-dependent glucose dehydrogenase (PQQ-GDH)-electrode with direct electron transfer based on polyaniline modified carbon nanotubes for biofuel cell application*, in Electrochimica Acta, Vol. 82 2012, Elsevier. p. 224-232. DOI: 10.1016/j.electacta.2012.03.128.

78. **Min, K., J.H. Ryu, and Y.J. Yoo,** *Mediator-free Glucose/O2 Biofuel Cell Based on a 3-Dimensional Glucose Oxidase/SWNT/Polypyrrole Composite* Electrode. Biotechnology and Bioprocess Engineering 2010. Vol. 15: p. 371-375. DOI: 10.1007/s12257-009-3034-z.

79. **Zebda, A., et al.,** *Mediatorless high-power glucose biofuel cells based on compressed carbon nanotube-enzyme electrodes.* Nature Communications, 2011. Vol.2(1): p. 370. DOI: 10.1038/ncomms1365.

80. **Dudzik, J., et al.,** *Cross-linked glucose oxidase clusters for biofuel cell anode catalysts.* Biofabrication, 2013. Vol. 5(3(035009)): p. 1-9. DOI: 10.1088/1758-5082/5/3/035009.

81. **Wen, D., et al.,** *A Membraneless Glucose/O2 Biofuel Cell Based on Pd Aerogels.* Electrocatalysis: European Journal., 2014. Vol. 20(15). DOI: 10.1002/chem.201304635.

82. **Deng, L., et al.,** *Multilayer structured carbon nanotubes/poly-L-lysine/laccase composite cathode for glucose/O2 biofuel cell.* Electrochemistry Communications 2008. Vol. 10(7): p. 1012–1015. DOI: 10.1016/j.elecom.2008.05.001.

83. **Scherbahn, V., et al.,** *Biofuel cells based on direct enzyme-electrode contacts using PQQ-dependent glucose dehydrogenase / bilirubin oxidase and modified carbon nanotube materials*. Biosensors and Bioelectronics, 2014. Vol. 61: p. 631-638. DOI: 10.1016/j.bios.2014.05.027.

84. **Kim, J. and K.-H. Yoo,** *Glucose oxidase nanotube-based enzymatic biofuel cells with improved laccase biocathodes.* Phys.Chem. Chem., 2013. Vol. 15(10): p. 3510-3517. DOI: 10.1039/C3CP00074E.

85. **Kwon, C.H., et al.,** *High-power biofuel cell textiles from woven biscrolled carbon nanotube yarns.* Nature Communications, 2014. Vol. 5: p. 3928 DOI: 10.1038/ncomms4928.

86. **Prasad, K.P., Y. Chen, and P. Chen,** *Three-Dimensional Graphene-Carbon Nanotube Hybrid for High-Performance Enzymatic Biofuel Cells.* Applied Materials & Interfaces, 2014. Vol. 6(5): p. 3387–3393. DOI: 10.1021/am405432b.

87. **Reuillard, B., et al.,** *High power enzymatic biofuel cell based on naphthoquinone-mediated oxidation of glucose by glucose oxidase in a carbon nanotube 3D matrix.* Phys.Chem. Chem. Phys., 2013. Vol. 15(14): p. 4892-4896. DOI: 10.1039/C3CP50767J.

88. **DeAngelis,** *K.M. Phosphate buffer*. Nebraska University, 2007. Online] 1 15, 2007. [Cited: 7 2, 2020.] Link: https://www.unl.edu/cahoonlab/phosphate%20buffer.pdf.

89. **B.Butler, I., M. A.A.Schoonen, and D. T.Rickard,** *Removal of dissolved oxygen from water: A comparison of four common techniques*. Talanta, 1994. Vol. 41 (2): p. 211-215. DOI: 10.1016/0039-9140(94)80110-X.

90. **I. Zekos and M.M.Stack,** *A note on a design protocol for deoxygenation of water.* Electrochemistry Communications, 2019. Vol. 103 p. 12-16. DOI: 10.1016/j.elecom.2019.04.009.

91. **Georgakilas, V., et al.,** *Noncovalent Functionalization of Graphene and Graphene Oxide for Energy Materials,* Biosensing, Catalytic, and Biomedical Applications. Chemical Reviews, 2016. Vol. 116(9): p. 5464–5519.

92. Georgakilas, V., Functionalization of Graphene. 2014: Wiley-VCH. DOI: 10.1002/9783527672790.

93. **McCreery, R.L. and K.K. Cline,** *Carbon Electrodes, in Laboratory Techniques* in Electroanalytical Chemistry, P. Kissinger; and W.R. Heineman;, Editors. 1996, Marcel Dekker Inc. p. 40. ISBN: 9780824794453.

94. **Bott, A.W., Pratical** *Problems in Voltammetry: 4.Preparation of working electrodes*, *Current Seperations* 1997: Bioanalytical Systems.

95. **Kamau, G.N.,** *Surface preparation of glassy-carbon electrodes*. Anal.Chim. Acta 207, 1988. Vol. 207: p. 1-16. DOI: 10.1016/S0003-2670(00)80777-1.

96. **Rezaei, B., M.H. Esfahani, and A.A. Ensafi,** *Modified Au Nanopraticles/imprinted Sol-gel/Multiwall Carbon Nanotubes Pencil Graphite Electrode as a selective Electrochemical sensor for papaverine determination*. Sens.J.16, 2016. Vol. 16(19): p. 7037 - 7044. DOI: 10.1109/JSEN.2016.2598381.

97. **N.Vishnu, et al.,** *Pencil graphite as an elegant electrochemical sensor for separation-free and simultaneous sensing of hypoxanthine, xanthine and uric acid in fish samples*. Anal. Methods 9, 2017. Vol. 9(15): p. 2265-2274. DOI: 10.1039/C7AY00445A:

98. **R. Deakin, M., K. J.Stutts, and R.M. Wightman**, *The effect of pH on some outer-sphere electrode reactions at carbon electrodes.* Journal of Electroanalytical Chemistry and Interfacial Electrochemistry, 1985. Vol. 182(1): p. 113-122. DOI: 10.1016/0368-1874(85)85444-7.

99. **Morrin, A., A.J. Killard, and M.R. Smyth,** *Electrochemical Characterization of Commercial and Home-Made Screen-Printed Carbon Electrodes*. Analytical Letters, 2007. Vol. 36(9): p. 2021-2039. DOI: 10.1081/AL-120023627.

100. **Nicholson, R.S.,** *Theory and application of the cyclic voltammetry of electrode reaction kinetics.* Anal. Chem., 1965. Vol. 37(11): p. 1351–1355. DOI: 10.1021/ac60230a016

101. **Pedersen, S.U. and K. Daasbjerg,** *Electrochemical Techniques, in Electron Transfer in Chemistry,* V. Balzani, Editor. 2001, Wiley. DOI: 10.1002/9783527618248.ch12.

102. **Jin, M., et al.,** *An electrochemical sensor for indole in plasma based on MWCNTs-chitosan modified screen-printed carbon electrode.* Biosensors and Bioelectronics, 2017. Vol. 98: p. 392-397. DOI: 10.1016/j.bios.2017.07.018.

103. **Babaeiab, A. and A.R.** *Taheria, Nafion/Ni(OH)2 nanoparticles-carbon nanotube composite modified glassy carbon electrode as a sensor for simultaneous determination of dopamine and serotonin in the presence of ascorbic acid.* Sensors and Actuators B: Chemical, 2013. Vol. 176 p. 543-551. DOI: 10.1016/j.snb.2012.09.021.

104. **Ausman, K.D., et al.,** *Organic Solvent Dispersions of Single-Walled Carbon Nanotubes:* Toward Solutions of Pristine Nanotubes. Physical Chemistry B 2000, 2000. Vol.104(38): p. 8911–8915. DOI: 10.1021/jp002555m.

105. **Kharissova, O.V., B.I. Kharisov, and E.G.d.C. Ortiz,** *Dispersion of carbon nanotubes in water andnon-aqueous solvents.* RSC Advances, 2013. Vol. 3: p. 24812-24852. DOI: /10.1039/C3RA43852J.

106. **Duan, W.H., F.G. Collins, and Q. Wang,** *Dispersion of carbon nanotubes with SDS surfactants: A study from a binding energy perspective.* Chemical Science 2011. Vol. 2(7): p. 1407-1413. DOI: 10.1039/C0SC00616E.

107. **Farehanim, M.A., et al.,** *Preparation and characterization of MWCNT dispersed in various solutions. I*EEE, 2014: p. 505-508. DOI: 10.1109/SMELEC.2014.6920909.

108. **Stetter, A.,** *Conductivity of Multiwall Carbon Nanotubes: Role of Multiple Shells and Defects.* Physical review. B, Condensed matter, 2011. Vol. 82(11). DOI: 10.1103/PhysRevB.82.115451.

109. **Iijima, S.,** *Helical microtubules of graphitic carbon.* Nature, 1991. Vol.354: p. 56-58. DOI: 10.1038/354056a0.

110. **Ogata, S. and Y. Shibutani**, *Ideal tensile strength and band gap of single-walled carbon nanotubes.* Physical Review B, 2003. Vol. 68(16): p. 165409. DOI: 10.1103/PhysRevB.68.165409.

111. **David, M.E., et al.,** *Nanomaterials Used in Conservation and Restoration of Cultural Heritage: An Up-to-Date Overview.* Materials, 2020. Vol. 13(9). DOI: 10.3390/ma13092064.

112. **Liu, C. and H.-M. Cheng,** *Carbon nanotubes: controlled growth and application.* MateriaslToday, 2013. Vol. 16 (1-2): p. 19-28. DOI: 10.1016/j.mattod.2013.01.019.

113. **S.RUOFF, R. and D. C.LORENTS,** *MECHANICAL AND THERMAL PROPERTIES OF CARBON NANOTUBES,* in Carbon Nanotubes, S. Iijima; and M. Endo;, Editors. 1996, Elsevier. p. 925-930. DOI: 10.1016/0008-6223(95)00021-5.

114. **Rafiee, M.A., et al.,** *Fracture and Fatigue in Graphene Nanocomposites.* Small, 2010 (2): p. 179-183. DOI: 10.1002/smll.200901480.

115. **Xuanying, L., et al.,** *Signal multi-amplified electrochemical biosensor for voltammetric determination of tau-441 protein in biological samples using carbon nanomaterials and gold nanoparticles to hint dementia.* Microchimica Acta, 2020. Vol. 187(302). DOI: 10.1007/s00604-020-04273-z.

116. **Opallo, M. and R. Bilewicz,** *Recent Developments of Nanostructured Electrodes for Bioelectrocatalysis of Dioxygen Reduction*. Advances in Physical Chemistry 2011. 2011 p. 1687-7985. DOI: 10.1155/2011/947637.

117. **M.A.Busch and K.W.Busch**, *BLEACHES AND STERILANTS,* in Encyclopedia of Analytical Science, **P. Worsfold**;, et al., Editors. 2005, Elsevier. p. 284-294.

118. **Huanga, Y.H., et al.,** *Effects of electrode area and interval on the sensitivity of bilateral silicon detectors used for neutron dosimetry*. Radiation Measurements, 2018. Vol. 119 p. 220-224. DOI: 10.1016/j.radmeas.2018.11.002.

119. **Massart, D.L., A. Dijkstra, and L. Kaufman,** *Techniques and Instrumentation* in Analytical Chemistry. Vol. 1. 1978: Elsevier. ISBN: 978-0-444-41743-5.

120. **Şengül, Ü.,** *Comparing determination methods of detection and quantification limits for aflatoxin analysis in hazelnut.* Journal of Food and Drug Analysis, 2016. Vol.24 (1): p. 56-62. DOI: 10.1016/j.jfda.2015.04.009.

121. **Zhang, Q.,** *Carbon nanotubes and their applications.* 2012: Pan Stanford Publishing. ISBN: 9789814241908.

122. **XM, W., et al.,** *Electrochemical Approach for Detection of Extracellular Oxygen Released from Erythrocytes Based on Graphene Film Integrated with Laccase and 2,2-Azino-bis(3-ethylbenzothiazoline-6-sulfonic acid).* Analytical chemistry, 2010. Vol. 82(9): p. 3588–3596. DOI: 10.1021/ac100621r.

123. **Palys, B., A. Bokun, and J. Rogalski**, *Poly-o-phenylenediamine as redox mediator for laccase.* Electrochimica Acta 2007. Vol. 52(24): p. 7075-7082. DOI: 10.1016/j.electacta.2007.05.029.

124. **Sandford, C., et al.,** *A synthetic chemist's guide to electroanalytical tools for studying reaction mechanisms.* Chemical Science, 2019. Vol. 10(26): p. 6404-6422. DOI: 10.1039/C9SC01545K.

125. **Zhanga, J., et al.,** *Carbon nanotubes coated with platinum nanoparticles as anode of biofuel cell.* Particuology, 2012. Vol. 10 (4): p. 450-455.DOI: 10.1016/j.partic.2011.11.014.

126. **Rothwel, S.A., S.J. Killoran, and R.D. O'Neill.,** *Enzyme Immobilization Strategies and Electropolymerization Conditions to Control Sensitivity and Selectivity Parameters of a Polymer-Enzyme Composite Glucose Biosensor.* Sensors (Basel), 2010. Vol. 10 (7): p. 6439-6462. DOI: 10.3390/s100706439.

127. **Guin, P.S., S. Das, and P.C. Mandal,** International Journal of Electrochemistry. 2011. 2011 (816202)(*Electrochemical Reduction of Quinones in Different Media: A Review*).

128. **Chakraborty, A., et al.,** *Impedance-based biosensors, in Bioelectronics and Medical Devices,* **K. Pal;, et al.,** Editors. 2019, WoodHead. p. 97-122. DOI: 10.1016/B978-0-08-102420-1.00005-4.

129. **Lee, H.-C., et al.,** *Development of Anodic Titania Nanotubes for Application in High Sensitivity Amperometric Glucose and Uric Acid Biosensors,* Sensors (Basel), 2013. Vol. 13 (10): p. 14161-14174. DOI: 10.3390/s131014161.

130. **Madhu, R., et al.,** *An enhanced direct electrochemistry of glucose oxidase at poly taurine modified glassy carbon electrode for glucose biosensor*. Analytical Methods, 2014. Vol. 6 (22): p. 9053-9058. DOI: 10.1039/C4AY01406E.

131. **Spiegel, C.,** *Polarization Curves*, in Fuel Cell Store. 2017. [Online] 6 20, 2017. [Cited: 6 25, 2020.]Link: https://www.fuelcellstore.com/blog-section/blogcat63/polarization-curves.

132. **Barbir, F.,** *Fuel cell Diagnostics,* in PEM Fuel Cells. 2005, Academic Press. p. 249-270.

133. **D.Parker, V.,** *Linear Sweep and cyclic voltammetry, in Electrode Kinetics: Principles and Methodology,* **C.H. Bamford; and R.G. Compton**;, Editors. 1986, Elsevier. p. 145-202. DOI: 10.1016/S0069-8040(08)70027-X.

134. **Agaesse, T.,** *Simulations of one and two-phase flows in porous microstructures, from tomographic images of gas diffusion layers of proton exchange membrane fuel cells.* 2016, l'Institut National Polytechnique de Toulouse

135. **S.Mischler and A.I.Munoz,** *Tribocorrosion,* in Encyclopedia of Interfacial Chemistry: Surface Science and Electrochemistry, K. Wandelt, Editor. 2018, Elsevier. p. 504-514.

136. **J.Geringer, et al.,** *Fretting corrosion processes and wear mechanisms in medical implants, i*n Bio-Tribocorrosion in Biomaterials and Medical Implants, **Y. Yan,** Editor. 2013, Woodhead Publishing. p. 45-73. DOI: 10.1533/9780857098603.1.45.

137. **D, K., et al.,** *Multi walled carbon nanotube and polyaniline coated pencil graphite based bio-cathode for enzymatic biofuel cell.* International Journal of Hydrogen Energy, 2015. Vol. 40(30): p. 9515-9522. DOI: 10.1016/j.ijhydene.2015.05.120.

138. **RP, R., et al.,** *High electrocatalytic activity of tethered multicopper oxidase-carbon nanotube conjugates.* Chemical Communications, 2010. Vol. 46(33): p. 6045-6047. DOI: 10.1039/C0CC00911C.

139. **Strack, G., et al.,** *Power Generation From a Hybrid Biological Fuel Cell* in Seawater. Bioresource Technology, 2012. Vol. 128: p. 222-228. DOI: 10.1016/j.biortech.2012.10.104.

140. **Lopez, R.J., et al.,** *Improved Interfacial Electron Transfer in Modified Bilirubin Oxidase Biocathodes.* ChemElectroChem, 2013. Vol. 1(1). DOI: 10.1002/celc.201300085.

141. **Karachevtsev, V.A., et al.,** *Noncovalent Interaction of Single-Walled Carbon Nanotubes with 1-Pyrenebutanoic Acid Succinimide Ester and Glucoseoxidase.* Physical Chemistry B 2000, 2011. Vol. 115(43): p. 21072–21082. DOI: 10.1021/jp207916d.

142. **Besteman, K., et al.,** *Enzyme-Coated Carbon Nanotubes as Single-Molecule* Biosensors. Nano Letters, 2003. Vol. 3(6): p. 727–730. DOI: 10.1021/nl034139u.

143. **Huang, Y., et al.,** *Nanoelectronic biosensors based on CVD grown graphene*. Nanoscale, 2010. Vol. 8(2): p. 1485-1488. DOI: 10.1039/c0nr00142b.

144. **Markoš, J.,** *Mass Transfer in Chemical Engineering Processes*. 2011: InTech. DOI: 10.5772/659.

145. **Jenkins, P., et al.,** *A comparison of glucose oxidase and aldose dehydrogenase as mediated anodes in printed glucose/oxygen enzymatic fuel cells using ABTS/laccase cathodes.* Bioelectrochemistry, 2012. Vol. 87: p. 172-177. DOI: 10.1016/j.bioelechem.2011.11.011.

146. **Fiorito, P.A. and S.I.C.d. Torresi,** *Glucose Amperometric Biosensor Based on the Co-immobilization of Glucose Oxidase (GOx) and Ferrocene in Poly(pyrrole) Generated from Ethanol / Water Mixtures.* Brazilian Chemical Society, 2001. Vol. 12(6). DOI: 10.1590/S0103-50532001000600007.

147. **Aurélien, H., et al.,** *Performances of Enzymatic Glucose/O2 Biofuel Cells,* in Biofuel's Engineering Process Technology, **M.A.D.S. Bernardes,** Editor. 2010, InTech Open. p. 467-492. DOI: 10.5772/17447.

148. **Habrioux, A., et al.,** *Concentric glucose/O2 biofuel cell.* Electroanalytical Chemistry, 2008. Vol, 622 (1): p. 97-102. DOI: 10.1016/j.jelechem.2008.05.011.

149. **Zhao, M., et al.,** *Mediatorless Glucose Biosensor and Direct Electron Transfer Type glucose/air Biofuel Cell Enabled With Carbon Nanodots.* Anal. Chem., 2015. Vol. 87(5): p. 2615-2622. DOI: 10.1021/acs.analchem.5b00012.